JGR Oceans

RESEARCH ARTICLE
10.1029/2024JC021670

An Asymmetric Change in Circulation and Nitrate Transports in the Bay of Bengal

J. E. Jardine[1], J. Holt[1], S. L. Wakelin[1], A. Katavouta[1], and D. Partridge[2]

[1]National Oceanography Centre, Liverpool, UK, [2]Plymouth Marine Laboratory, Plymouth, UK

Key Points:

- We use a nonprobabilistic, storyline approach to investigate mechanistic changes in the Bay of Bengal under an idealized climate scenario
- Circulation around the Bay of Bengal exhibits an asymmetrical response to climate change
- Surface nitrate transports decrease by 14% in the northern Bay of Bengal and increase by 52% in the southern Bay of Bengal

Supporting Information:

Supporting Information may be found in the online version of this article.

Correspondence to:

J. E. Jardine,
jenjar@noc.ac.uk

Citation:

Jardine, J. E., Holt, J., Wakelin, S. L., Katavouta, A., & Partridge, D. (2025). An asymmetric change in circulation and nitrate transports in the Bay of Bengal. *Journal of Geophysical Research: Oceans*, *130*, e2024JC021670. https://doi.org/10.1029/2024JC021670

Received 31 JUL 2024
Accepted 10 JAN 2025

Author Contributions:

Conceptualization: J. E. Jardine
Formal analysis: J. E. Jardine
Funding acquisition: J. Holt
Investigation: J. E. Jardine, J. Holt, S. L. Wakelin
Methodology: J. E. Jardine, J. Holt, S. L. Wakelin, A. Katavouta, D. Partridge
Project administration: J. Holt
Supervision: J. Holt, S. L. Wakelin
Validation: J. E. Jardine
Visualization: J. E. Jardine
Writing – original draft: J. E. Jardine
Writing – review & editing: J. E. Jardine, J. Holt, S. L. Wakelin

Abstract The Bay of Bengal is a dynamic region that experiences intense freshwater runoff, extreme meteorological events, and seasonally reversing surface currents. The region is particularly susceptible to anthropogenic climate change, driven in part by large air-sea fluxes, persistent freshwater stratification, and low overturning rates. Predicting how this system is likely to change in the future is paramount for planning effective adaption and mitigation strategies. Using a relocatable, coupled physics-ecosystem regional coastal ocean model (NEMO-ERSEM), we investigate potential future changes in surface circulation and coastal nitrate pathways around the coast of the Bay of Bengal from 1980 to 2060, using a "business-as-usual" climate change scenario. We find that future surface currents are reduced in the northern Bay of Bengal (summer) and strengthened in the southern Bay of Bengal (fall). Coastal nitrate transports mirror this asymmetric change and decrease by as much as 14% in the northern Bay of Bengal, perpetuating a positive feedback loop whereby the northern Bay of Bengal becomes progressively fresher and more nutrient-rich, strengthening surface stratification and increasing the risk of toxic algal blooms and eutrophication events. Conversely, in the southern Bay of Bengal, coastal nitrate transports increase by 52% that promotes localized diatom blooms despite reduced regional river runoff. This work highlights the need for more rigorous scenario testing in the region and presents new challenges for mitigating the impact of anthropogenic climate change across South Asia.

Plain Language Summary The Bay of Bengal is bordered by some of the largest rivers in the world, including the Ganges and Irrawaddy rivers. The huge input of fresh, high-nutrient river water influences physical and ecological processes within the Bay of Bengal, making the region more susceptible to the effects of climate change. Using numerical simulations that include both physical and ecosystem interactions, we compared the near-present day (1990–2010) conditions in the Bay of Bengal of Bengal to a predicted future (2040–2060) that includes the "business-as-usual" trend of global warming. We found that different regions of the Bay of Bengal responded differently to this predicted climate scenario. In the northern Bay of Bengal, reduced surface ocean currents, combined with a higher amount of river runoff, resulted in the northern Bay of Bengal becoming progressively fresher. Conversely, surface ocean current speeds increased along the southeastern Indian coast, boosting local marine algal growth as more nutrients were transported in from other coastal areas. This research highlights the need for more ocean simulations in the Bay of Bengal of Bengal across a range of future climate change scenarios, and will help govern the direction of future policy changes to mitigate the effects of climate change across the region.

1. Introduction

Semienclosed by India to the west, Bangladesh to the north, and Myanmar to the east, the Bay of Bengal (the Bay) is a dynamic region that is heavily influenced by seasonal changes in wind and river forcing. The Bay of Bengal receives approximately 1.625×10^{12} m^3 of river runoff per year (Subramanian, 1993), making it the freshest region in the Indian Ocean. The resulting cap of surface freshwater, combined with the high precipitation rates (2 m yr^{-1}; Gill, 1982; Prasad, 1997) and air temperatures, leads to strong near-surface density stratification (Han et al., 2001; Prasad, 1997; Rao & Sivakumar, 2003) and the formation of a barrier layer (Girishkumar et al., 2011; Thadathil et al., 2007; Vinayachandran et al., 2002), which traps heat below the surface mixed layer. Consequently, diapycnal mixing is inhibited, resulting in oligotrophic conditions. The injection of new nutrients into the Bay of Bengal, via increased diapycnal mixing from cyclones and tropical storms (e.g., Kuttippurath et al., 2021; Maneesha et al., 2011; Vinayachandran, 2009), or from riverine nutrients, is thus essential for promoting and sustaining primary production across the region (e.g., Gomes et al., 2000; Mishra et al., 2009; Vidya et al., 2017).

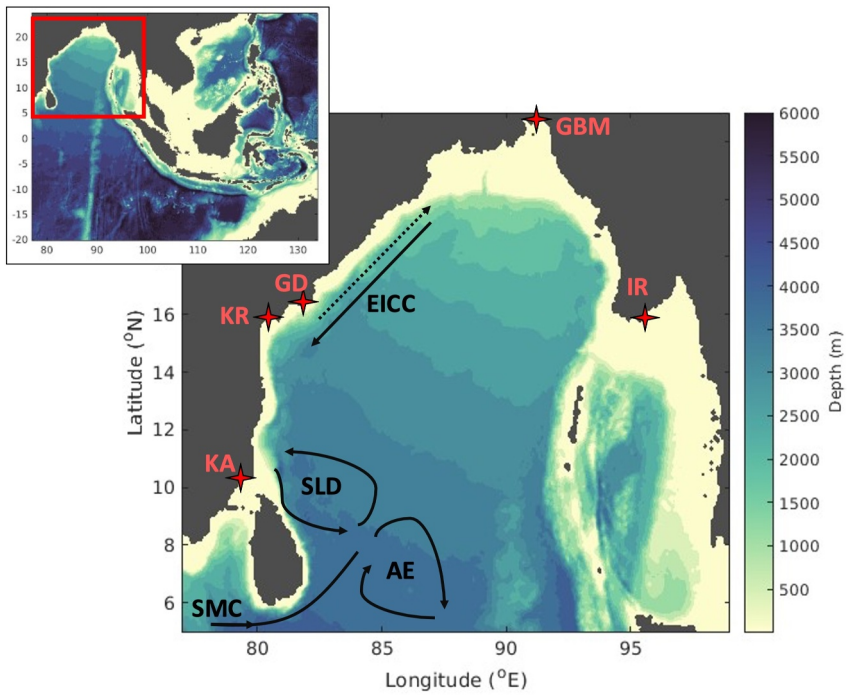

Figure 1. Bathymetry map (m; ORCA12) of the entire SEAsia model domain (insert), along with a zoomed-in bathymetry map of the Bay of Bengal (as indicated by the red box). Black arrows indicate the current direction in the summer monsoon (solid lines) and winter monsoon (dashed line; EICC only). The current names are as follows: EICC, East Indian Coastal Current; SLD, Sri Lanka Dome; AE, anticyclonic eddy; and SMC, Southwest Monsoon Current. The red stars indicate the position of major rivers around the Bay of Bengal: IR, Irrawaddy River; GBM, Ganges-Brahmaputra-Meghna Delta; GD, Godavari River; KR, Krishna River; and KA, Kaveri River.

Annually, rivers export 1.74 Tg of nitrate, 0.27 Tg of phosphate, and 3.58 Tg of silicate (Krishna et al., 2016) into the Bay of Bengal. The high-nutrient river runoff is largely constrained to the coastal seas by geostrophy (Amol et al., 2020) and transported around the Bay of Bengal by seasonally reversing surface currents. An anticyclonic flow occurs during the Northern Hemisphere winter (northeast) monsoon, followed by a cyclonic flow during the summer (southwest) monsoon (Potemra et al., 1991). The East Indian Coastal Current (EICC) helps regulate the salinity of the Bay of Bengal through the exchange of saline water from the Arabian Sea (Prasanna Kumar et al., 2004; Rainville et al., 2022; Sanchez-Franks et al., 2019; Trott et al., 2019), as well as facilitating the exchange of nutrients from the Bay of Bengal to the Arabian Sea, triggering localized biological production (Prasanna Kumar et al., 2004). The EICC is modulated by the Sri Lanka Dome (SLD), a region of cyclonic circulation to the east of Sri Lanka (Figure 1) that forms when the Summer Monsoon Current (SMC) turns northeast into the Bay of Bengal (Cullen & Shroyer, 2019; de Vos et al., 2014; Vinayachandran & Yamagata, 1998). The SLD, along with a paired anticyclonic eddy (AE) that forms to the west of the SMC, is highly variable as its position, longevity, and evolution is constrained by the local wind stress curl during the summer monsoon (Cullen & Shroyer, 2019). On average, the SLD forms during June–July, propagates northward, and dissipates during September (Cullen & Shroyer, 2019; Vinayachandran & Yamagata, 1998).

Riverine nutrients account for 17% of the total primary production in the Bay of Bengal (Krishna et al., 2016). However, excessive amounts of nutrients in river runoff, mostly from anthropogenic activity (Kumar et al., 2022; Rabalais et al., 2009), can alter the local nutrient stoichiometry (Islam et al., 2004; Tripathy et al., 2005) and can trigger harmful algal blooms (HABs; Naik et al., 2011; Sahu et al., 2014) and eutrophication events (Sattar et al., 2014) that negatively impact fisheries, human health, and tourism (e.g., Bricker et al., 2008). As nutrient input into the Bay of Bengal is expected to double by 2050 (Sattar et al., 2014), understanding how this nutrient-rich river runoff will be seasonally distributed around the Bay of Bengal is an essential step in developing measures to mitigate the impact of anthropogenic climate change in coastal environments.

Predicting future conditions in the Bay of Bengal is further complicated through predicted changes to regional precipitation and wind. An example is the precipitation-wind paradox (Ueda et al., 2006), where it is predicted that future wind speeds across the region will be reduced, but precipitation will increase due to the land-sea thermal contrast (Ma & Yu, 2014). Monsoon circulation is expected to decrease by as much as 14% per century (Dash et al., 2015; Goswami et al., 2022; Tanaka et al., 2004) and Saha et al. (2017) reported up to a 3% decrease in the CMIP5 RCP8.5 projected wind speeds compared to the 1996–2005 mean and an increase in precipitation predicted by CMIP5 and CMIP6 models. Furthermore, Sharmila et al. (2015) and Ha et al. (2020) predicted a delayed retreat of the summer monsoon in future climates, with consequences for circulation and nutrient redistribution around the Bay of Bengal.

Regional ocean models allow the development of understanding the consequences of these changes by exploring detailed physical-biogeochemical interactions under future climate forcing. Downscaling allows for the addition of fundamental processes, for example, tides, that are only fully resolved at higher spatial resolutions and more frequent time steps but at greater computational cost (Drenkard et al., 2021). As such, we use a single projection of a coupled physics-ecosystem ocean model as a mechanistic study to investigate the potential impact future changes in the hydrology and wind forcing could have on the Bay of Bengal. We further use this to contextualize the changes in circulation and associated nutrient transport across two contrasting time periods (1990–2010 and 2040–2060). Results from this study will help better understand the potential future evolution of nitrate transports and inferred biogeochemical cycling across the region.

2. Methods

The Southeast Asia model (SEAsia; Figure 1) is a 1/12th-degree (~9-km) resolution regional configuration of the Nucleus for European Modeling of the Ocean (NEMO version 3.6; Madec et al., 2017) covering much of the eastern Indian Ocean (20°S to 24°N, 77°E to 134°E). For the purposes of this study, we only focus on the Bay of Bengal of Bengal region (red box in Figure 1). The model has 75 vertical levels that use a hybrid σ-z* coordinate scheme (Luneva et al., 2015), whereby z* coordinates with partial steps are employed in the open ocean (in regions where depth >430 m), and terrain following σ coordinates are used in shallower regions (<430 m) as this maintains resolution in shallower water and better represents bottom boundary layers, without introducing hydrostatic pressure gradient errors (Wise et al., 2022). Minimum and maximum model depths are 10 and 6,000 m respectively. The model uses ORCA12 bathymetry (DRAKKAR Group, 2007).

The model employs a time-splitting method with a baroclinic time step of 360 s and a barotropic time step chosen as to satisfy a maximum Courant number of 0.5, and a nonlinear free surface is implemented using the variable volume layer scheme (Levier et al., 2007). A Laplacian lateral eddy diffusion scheme with a coefficient of 125 $m^2\ s^{-1}$ is used for tracers, and a bi-Laplacian lateral eddy viscosity scheme with a coefficient of $1.25 \times 10^{10}\ m^4\ s^{-1}$ is used for momentum. The generic length scale turbulent closure scheme (Umlauf & Burchard, 2003) with a k-ϵ predefined turbulence model and the Canuto et al. (2001) stability function is used for the parameterizations of vertical diffusion of tracers and momentum. Barotropic velocities and sea surface height are introduced to the model using the Flather radiation condition (Flather, 1994), while the baroclinic velocities are specified along the open lateral boundaries. These parameterizations and closure schemes were tested as a part of a series of sensitivity experiments in the region (Katavouta et al., 2022).

For the climate simulation (SEAsia Climate), atmospheric forcing is sourced from the HadGEM2 (CMIP5) run that considers the "business as usual" RCP8.5 emissions scenario. Lateral boundary and initial conditions are taken from the global 1/4° NEMO-MEDUSA ROAM simulation using identical surface forcing (see Yool et al., 2015). The model includes 34 tidal constituents (FES2014 tide model; Lyard et al., 2021), applied as a tidal potential and as a sea surface height and barotropic currents along the model's open lateral boundaries. River forcing was generated using the GlobalNEWS2 model (Beusen et al., 2009; Mayorga et al., 2010; Seitzinger et al., 2010) with constant land use and hydrology from the GlobalNEWS2 Realistic Hydrology 2000 (data set version 1.0. 12-11-2014), but varying precipitation from the HadGEM2 atmospheric forcing. GlobalNEWS2 generates annual river discharge and dissolved organic and inorganic nitrate concentrations, which we convert to monthly values based on weighted averages. The GlobalNEWS2 output was mapped onto the SEAsia grid; due to the coarser resolution of the GlobalNEWS2 grid (1/2°), river mouth locations were manually checked to ensure they were correctly mapped onto the model grid, and any rivers deemed too close to boundaries were removed. In total, 511 rivers were included in the SEAsia Climate model run. Discharge from 11 large rivers, including the

Ganges and Irrawaddy, were evenly spread along the coastline around the river mouth to improve model stability, and all runoff in the model was mixed across the top 10 m at the river mouth locations. The SEAsia Climate model is coupled to the biogeochemical model ERSEM (European Regional Seas Ecosystem Model; Baretta et al., 1995; Blackford et al., 2004; Butenschön et al., 2016), using the FABM coupler (Bruggeman & Bolding, 2014). Full details on the biogeochemical model set up can be found in Partridge (2022).

Following an initial spin-up period of 20 years (1960–1980), the SEAsia Climate model was run from 1980 to 2060. Temperature (°C) and salinity (PSU) were outputted as 5-day averages, and velocities (U and V; ms^{-1}), nitrate (mmol m^{-3}), and phytoplankton biomass (mg C m^{-3}) were outputted as monthly variables. Phytoplankton are split into diatoms (silicate utilization), microphytoplankton (>20 μm), nanophytoplankton (2–20 μm), and picophytoplankton (<2 μm). More details on the food web metrics and dependencies in ERSEM can be found in Butenschön et al. (2016). For the analysis considered here, all variables were averaged across the top 25 m of the water column as this depth range best encompassed the surface currents and the vertical extent of the river runoff. A particular caveat of this model experiment is that only a single future climate scenario is considered, in terms of driving both the global model and greenhouse gas emissions. This implies that, while we present a single consistent and plausible view of the future, we can make no comment on the likelihood of it occurring.

SEAsia Climate model data from 1980 to 2023 was compared to an annual gridded climatology for temperature and salinity (0.25° *x* 0.25° grid; 1981 to 2023) and nitrate concentrations (1° *x* 1° grid; 1990–2023), downloaded from the World Ocean Atlas 2023 (WOA, WOA23; Mishonov et al., 2024). Model data were interpolated onto the WOA grid for direct comparisons, and any WOA grid cells containing less than two observational points were discarded. To further assess the SEAsia Climate model, we compare with a physics-only hindcast model run (SEAsia Hindcast) that runs from 1980 to 2012, and the NEMO-MEDUSA model (ROAM; Yool et al., 2015; 1980–2023) that was used for the initial and boundary conditions. The SEAsia Hindcast model (Katavouta et al., 2022) uses the same model grid as SEAsia Climate, and atmospheric forcing from the ERA5 reanalysis, and initial and boundary conditions from the CMS GLORYSVS reanalysis data set (see Katavouta et al., 2022). Satellite sea surface temperature (Level 4 SST CCI product, 0.05° resolution; Embury et al., 2024), chlorophyll concentrations (Level 3 merged data set V5.0; Sathyendranath et al., 2021), and OSCAR surface currents (Level 4 Final V2.0, 0.25° grid resolution; ESR et al., 2022) were also used as validation data sets. HadGEM2 data (wind speed and precipitation) used to force SEAsia Climate model was validated against ERA5 data and can be found in the Supporting Information S1.

Following Chatterjee et al. (2012), seasonal means were calculated to better represent the monsoonal dynamics in the region: spring (MAM), summer (JJAS), fall (ON), and winter (DJF).

3. Results

3.1. Validation

Average Bay of Bengal temperatures from 0 to 25 m across the SEAsia Climate, the SEAsia Hindcast, and the ROAM models are cooler than the WOA observations (Figure 2). The SEAsia Hindcast model (Figure 2a) has the lowest average temperature bias across the region (−0.17°C), while SEAsia Climate (Figure 2b) and ROAM (Figure 2c) have comparable biases of −0.69°C and −0.62°C, respectively, with the largest temperature differences located in the northwest part of the region. Average RMSE (Figures 3a–3c) values for SEAsia Hindcast, SEAsia Climate, and ROAM are 0.68°C, 1.07, and 1.03°C, respectively. Comparing the seasonal climatology of the models to WOA observations reveals a similar cold bias across all seasons in SEAsia Climate and ROAM, but a predominantly warm bias in Spring (MAM) in SEAsia Hindcast (Figure S1 in Supporting Information S1), which is also seen when comparing to SST satellite data (Figure S2 in Supporting Information S1). Figure 4 shows the average monthly temperatures across the Bay of Bengal region for all three models, and in all cases, monthly temperatures (light gray lines) follow the observed cycle (red line) and suggests all models are capturing the mean annual conditions within the Bay of Bengal despite high interannual variability. Temperature profiles averaged across the Bay of Bengal (Figure S3 in Supporting Information S1) indicate how well the models replicate temperature at depth, and show that SEAsia Hindcast has better agreement to the observed thermocline from 150 to 400 m compared to SEAsia Climate; however, the overall shape of the thermocline remains consistent between both models. Furthermore, although profiles (SEAsia Hindcast and SEAsia Climate) have better agreement to observations nearer the surface, they are still within a 2°-C difference at a 25-m depth across all seasons (Figure S4 in Supporting Information S1).

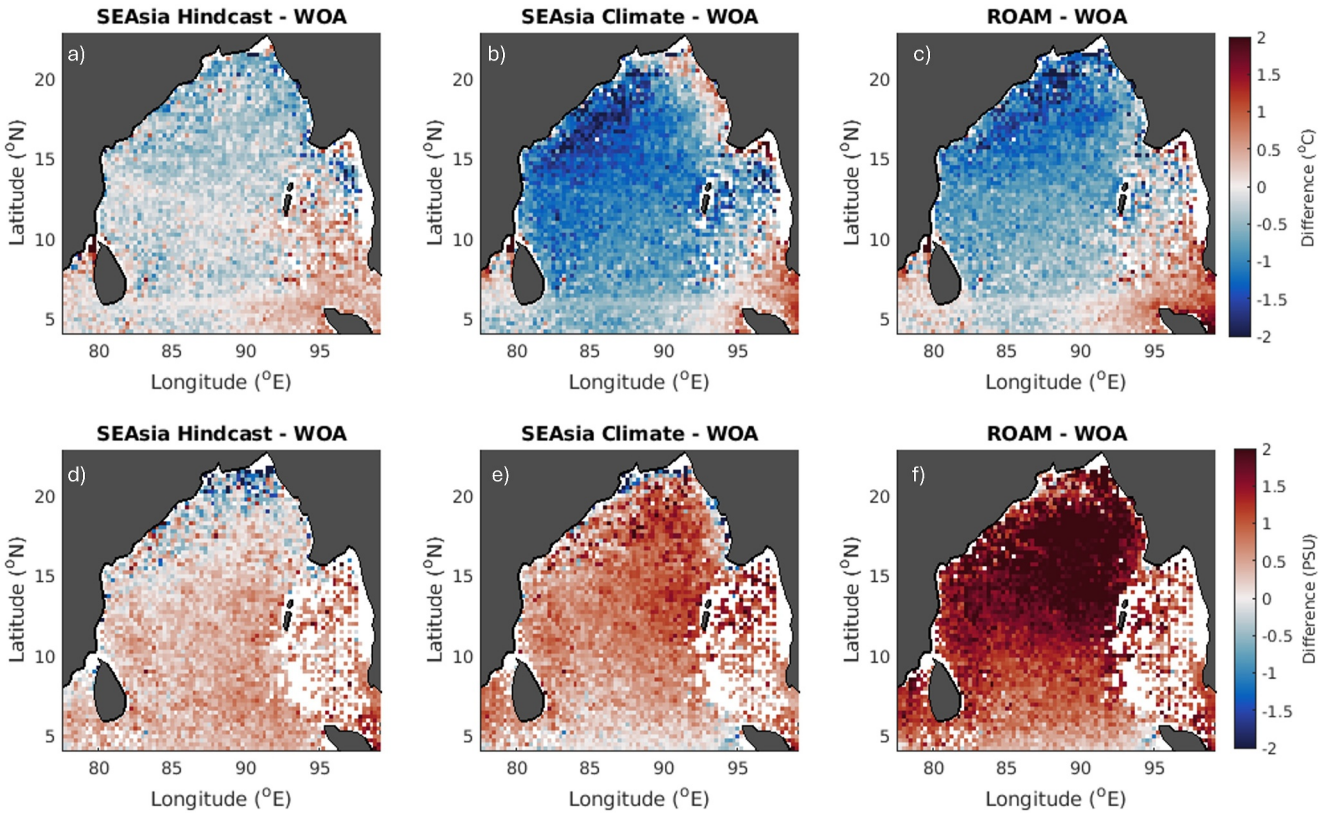

Figure 2. Spatial biases of temperature (top row; °C) and salinity (bottom row, PSU) compared to WOA23 observations, for the SEAsia Hindcast model (1980–2012), SEAsia Climate model (1980–2023), and the ROAM model (1980–2023). All model data have been interpolated onto the WOA23 grid, and grid cells with <2 observations have been discarded.

The average salinity bias in SEAsia Climate (Figure 2e) is an intermediate value (0.52) between the salinity bias in SEAsia Hindcast (0.01) and ROAM (1.55). The large salinity bias in ROAM (Figure 2f) in the central and the northern part of the Bay of Bengal is likely due to discrepancies in the riverine freshwater fluxes, or through shared bias from the ROAM sea surface salinity relaxation to the HadGEM-ES (occurs every 30 days; Yool et al., 2015). However, this salinity bias was reduced in SEAsia Climate due to the 20-year spin-up period to equilibrate the system. The respective regional-averaged RMSE values (Figures 3d–3f) for SEAsia Hindcast (0.83), SEAsia Climate (0.99), and ROAM (1.64) further demonstrate that SEAsia Climate performs better than ROAM at reproducing salinity, and that high salinity values from the ROAM boundaries do not propagate into the central Bay of Bengal, even during spring and winter where the ROAM salinity bias is most pronounced (Figure S5 in Supporting Information S1). Monthly changes in salinity for the SEAsia models follow observations (Figure 4); however, SEAsia Climate is on average 0.49 more saline than SEAsia Hindcast (0.13). Nevertheless, SEAsia Climate is still able to reproduce the monthly salinity cycle, and greatly improves on the ROAM salinity, which is ∼1.56 higher than observations. When comparing the models' ability to replicate salinity across the top 0–800 m, salinity-depth profiles (Figures S3e–S3j in Supporting Information S1) show high agreement between SEAsia Hindcast and observations, and SEAsia Climate salinity profiles only show <0.5PSU difference over the top 600 m.

Mean surface currents from SEAsia Hindcast and SEAsia Climate are consistently higher in the central Bay of Bengal than the observed currents recorded by OSCAR satellites (Figure 5). Nevertheless, the direction and position of the EICC remains consistent with satellite currents. Both SEAsia models replicate the stronger currents in the southeastern part of the Bay of Bengal and thus perform better than ROAM; however, the spread and magnitude of the currents are still more than observations. Furthermore, SEAsia Climate shows stronger cyclonic and anticyclonic rotation along the southern coast of India and Sri Lanka. As the anticyclonic rotation is more strongly presented in the ROAM model, and not present in SEAsia Hindcast, and given the proximity of Sri Lanka to the boundary, it can be assumed the stronger eddies in SEAsia Climate result from boundary forcing conditions

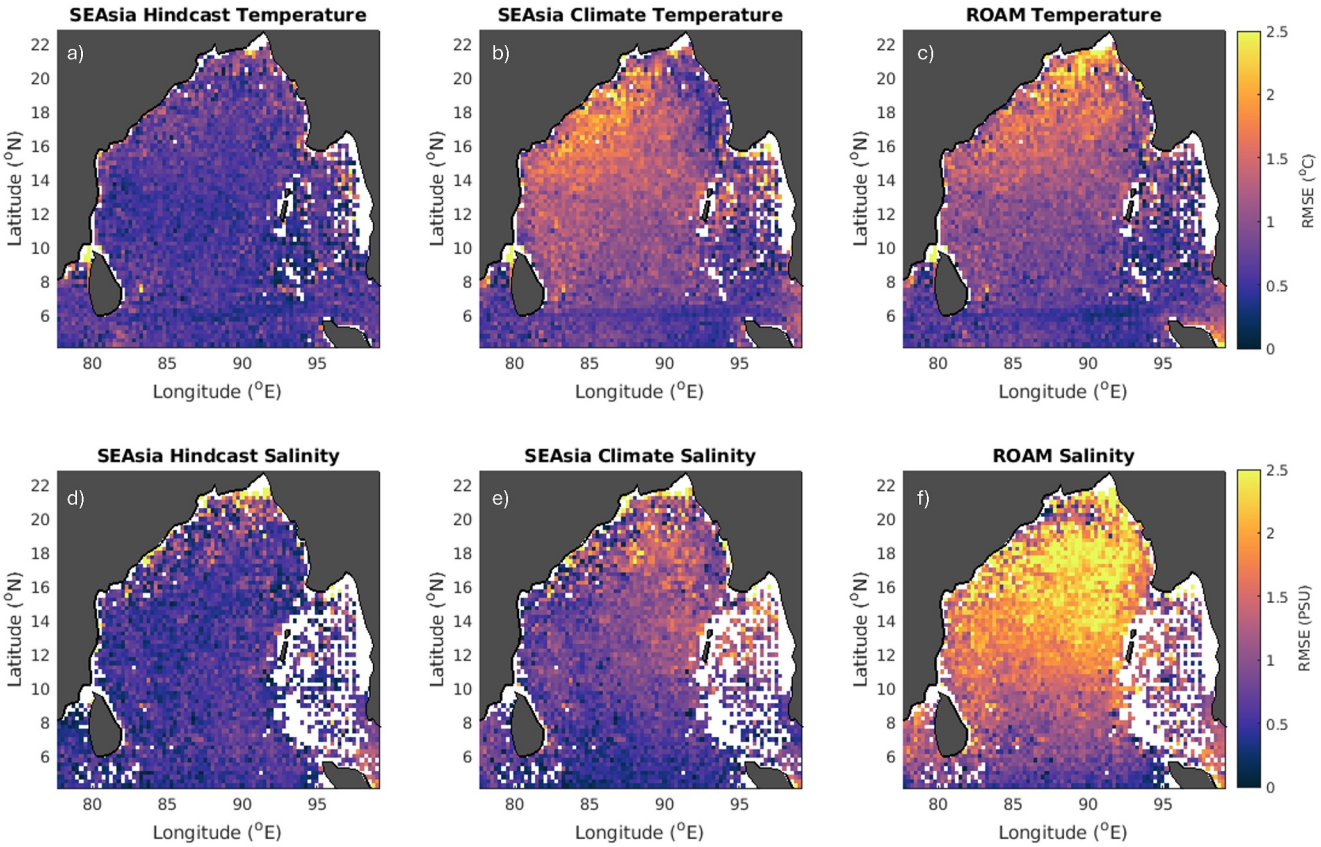

Figure 3. Spatial RMSE for the monthly temperature (top row; °C) and salinity (bottom row, PSU) climatology compared to WOA23 observations, for the SEAsia Hindcast model (1980–2012), the SEAsia Climate model (1980–2023), and the ROAM model (1980–2023). All model data have been interpolated onto the WOA23 grid, and grid cells with <2 observations have been discarded.

from ROAM. Nevertheless, the position of the fall intermonsoon cyclonic/anticyclonic currents in SEAsia Climate are two degrees further south than ROAM and are more consistent with the position of the cyclonic rotation seen in OSCAR data. The discrepancies between the SEAsia Climate versus the OSCAR currents can be explained by the distribution of the maximum (>7 ms^{-1}) wind speeds in HadGEM2, which are located to the east of Sri Lanka and extend over much of the Bay of Bengal, whereas maximum wind speeds in ERA5 are concentrated around the southern tip of India, including Sri Lanka, and are 0.5 ms^{-1} lower than HadGEM2 in the Bay of Bengal's interior (Figure S6 in Supporting Information S1). Monthly wind speeds and precipitation from HadGEM2 for the Bay of Bengal are comparable with the ERA5 climatology (Figures S7 and S8 in Supporting Information S1).

Due to the limited number of nitrate observations, no spatial comparisons were done. Instead, direct comparisons of seasonal SEAsia Climate nitrate concentrations were made to WOA23 nitrate concentrations from 0 to 800 m (Figure 6) and show good agreement (average R value of 0.92). Summer shows the largest deviation from observations ($R = 0.84$). To gauge how well SEAsia Climate reproduces the changing nitrate concentrations with depth, model nitrate concentration profiles were compared to WOA23 observations, averaged across the Bay of Bengal. SEAsia Climate nitrate profiles from 0 to 800 m for summer (Figure S3l in Supporting Information S1) show the most deviation from observations below 250-m depth; however, the model still captures the depth of the nitracline across all seasons. Near the surface (<25 m), biases in SEAsia Climate nitrate concentrations are consistently less than 1.5 mmol N m^{-3} across all seasons (Figures S4k–SKn in Supporting Information S1), and can be attributed to interannual variations in river nutrient runoff, and uncertainties in the river model used for the model experiment. For the purposes of this study, modeled variations in the near-coastal nitrate concentrations are acceptable considering we are investigating how the region could change in a highly idealized climate scenario. Furthermore, this extensive validation reveals that while the SEAsia Climate run agrees less well with

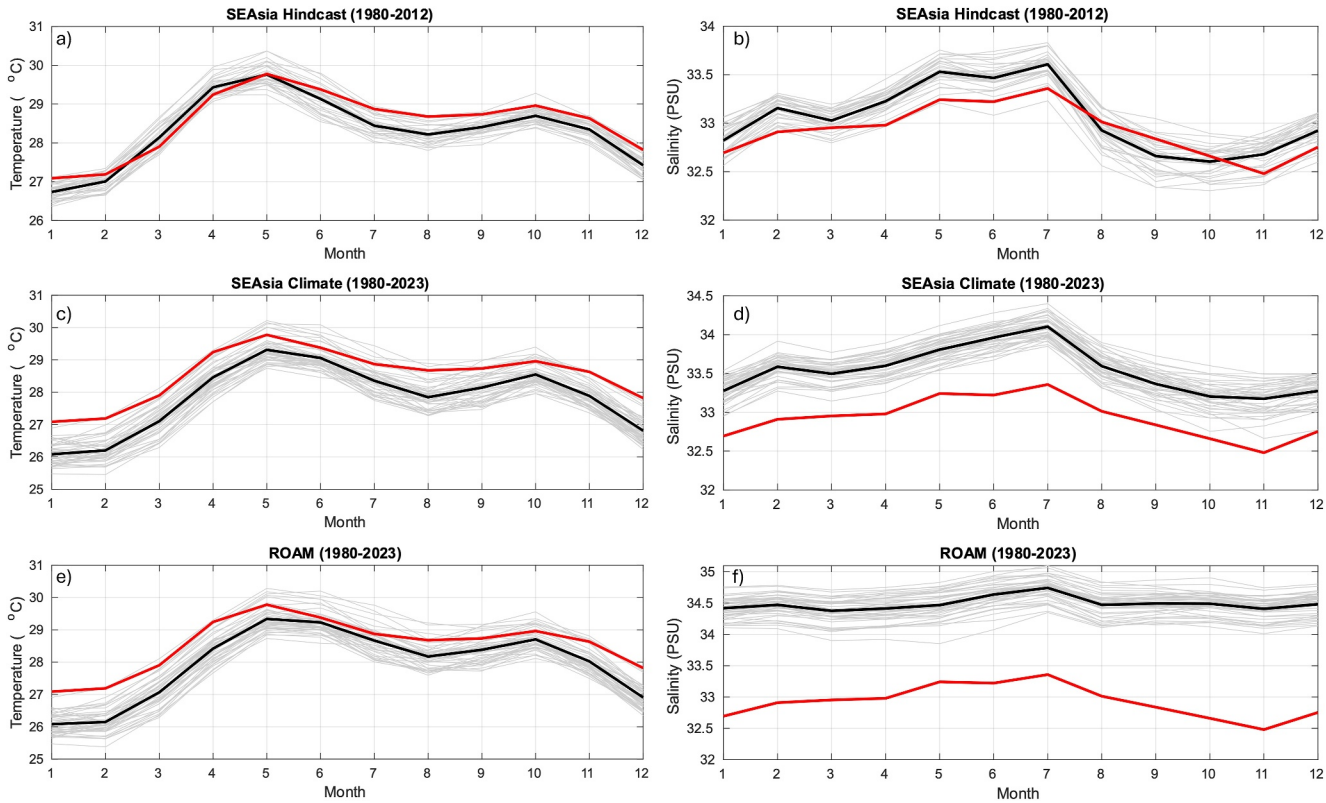

Figure 4. Monthly temperature (left; °C) and salinity (right; PSU) climatology (black lines) for the SEAsia Hindcast (1980–2012), the SEAsia Climate model (1980–2023), and the ROAM global model. The gray lines are the monthly averages for each year to show the interannual variability, and the red lines show the temperature/salinity climatology from the WOA23 data. All data have been averaged across the Bay of Bengal.

observations when compared to a SEAsia Hindcast run, it is still within acceptable limits and markedly improves upon deficiencies in the ROAM global model.

No observational measurements of phytoplankton biomass were available. Instead, we compared the SEAsia Climate model to satellite chlorophyll measurements to compare the seasonal evolution of modeled phytoplankton biomass to the distribution of surface chlorophyll. The comparison (Figure S9 in Supporting Information S1) indicates the model can reproduce the seasonal evolution of phytoplankton, with lowest values occurring in the spring (MAM), and highest phytoplankton biomass in the interior of the Bay of Bengal occurring during the summer monsoon (JJAS). Similar to the spatial distribution of satellite chlorophyll, modeled phytoplankton biomass is most strongly concentrated near the coasts, especially in the northern Bay of Bengal. Despite this, modeled phytoplankton biomass is lower than values implied by the satellite chlorophyll concentrations in the northeastern Bay of Bengal, most noticeably during spring and summer, and particularly offshore from the Myanmar coast. Such discrepancies could be due to limitations of the model in reproducing phytoplankton in this area but could equally be due to limitations of satellites in capturing chlorophyll concentrations only at the surface. Nevertheless, as this is a mechanistic study using a specific climate scenario, the model's ability to replicate changes in phytoplankton biomass resulting from changes in the underlying physics is sufficient.

3.2. Past Versus Future Changes

From the past (1990–2010) to the future (2040–2060) time slices (hereafter defined as future minus past and denoted by the subscript F–P), seasonally averaged modeled temperatures across the Bay of Bengal increase by >1°C across all seasons (Figure 7), with the maximum increase (+2.4°C) occurring in the northeast Bay of Bengal during the winter. While future temperatures peak at 32.7°C during summer, the largest significant change in future temperatures ($T_{F\text{-}P}$) occurs during winter and spring, suggesting these seasons are the most vulnerable to climate change. Winter shows minimum temperatures of 20.2 and 22.1°C for the past and future, respectively, and

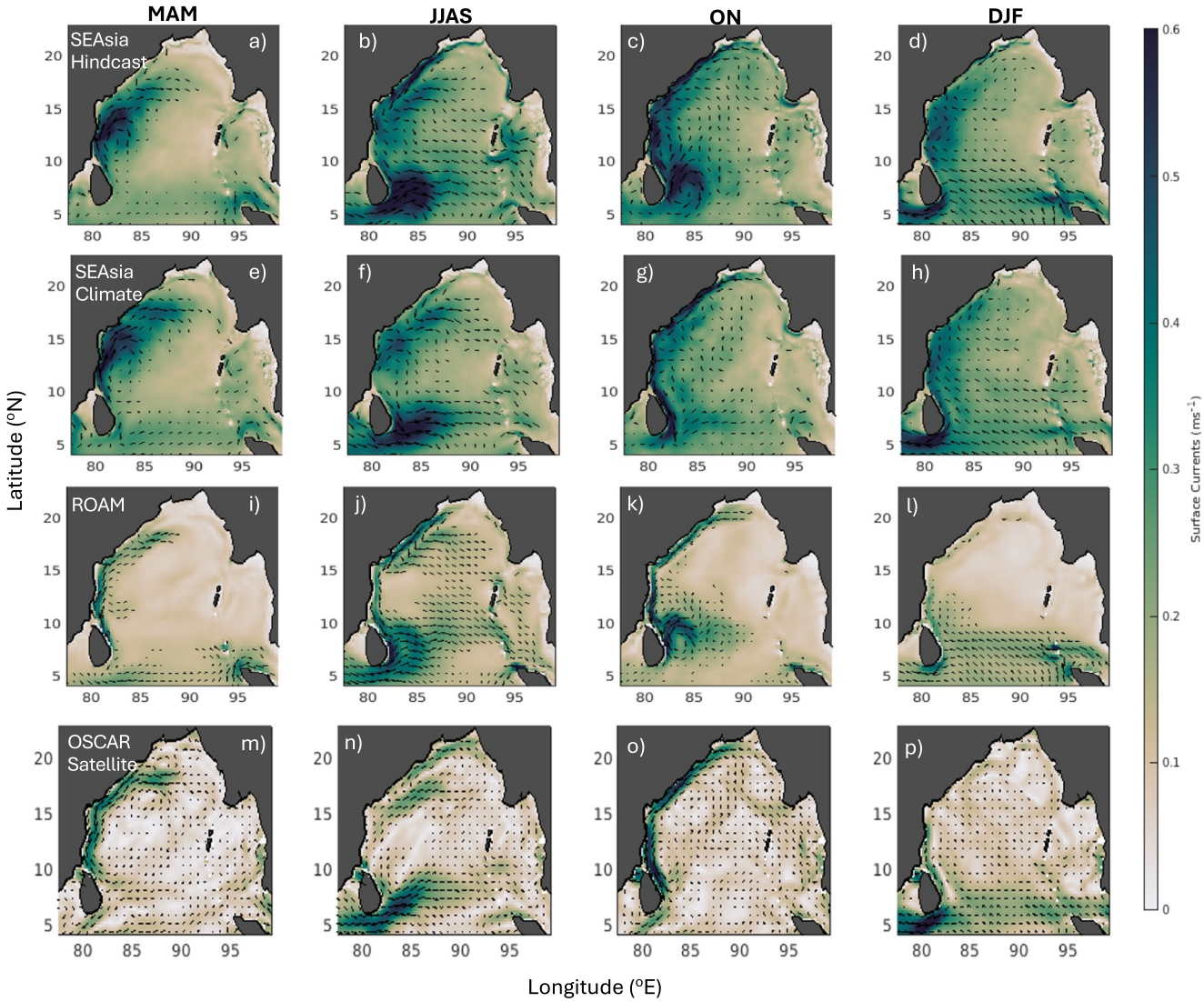

Figure 5. Surface mean current speed (ms^{-1}; color map) for the SEAsia Hindcast model (a–d), SEAsia Climate (e–h), ROAM (i–l), and from the OSCAR satellite (m–p). Seasonal averages are denoted by the following columns: left: spring (MAM); left-middle: summer (JJAS); right-middle: fall (ON); and right: winter (DJF). Current direction is denoted by the black quiver plot; to help identify to main currents, currents with speeds <0.175 ms^{-1} have been omitted in SEAsia Hindcast and SEAsia Climate quiver plots, and speeds <0.125 ms^{-1} omitted in the ROAM and OSCAR quiver plots. The resolution of the data for the current direction has also been cut for figure clarity, with black arrows plotted for every 12th grid point in SEAsia Hindcast and SEAsia Climate, and every 3rd grid point in ROAM and OSCAR.

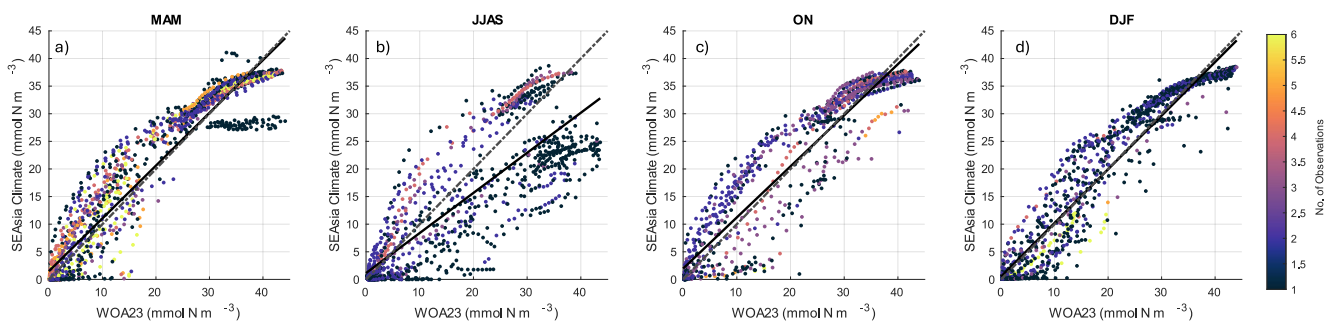

Figure 6. Direct comparisons between the WOA23 nitrate concentrations and the SEAsia Climate nitrate concentrations across the Bay of Bengal, from 0 to 800 m, including the linear regression (solid black line) and the one-to-one relationship (dashed gray line) for (a) MAM, (b) JJAS, (c) ON, and (d) DJF. The colored dots indicate the number of WOA23 observations at each point.

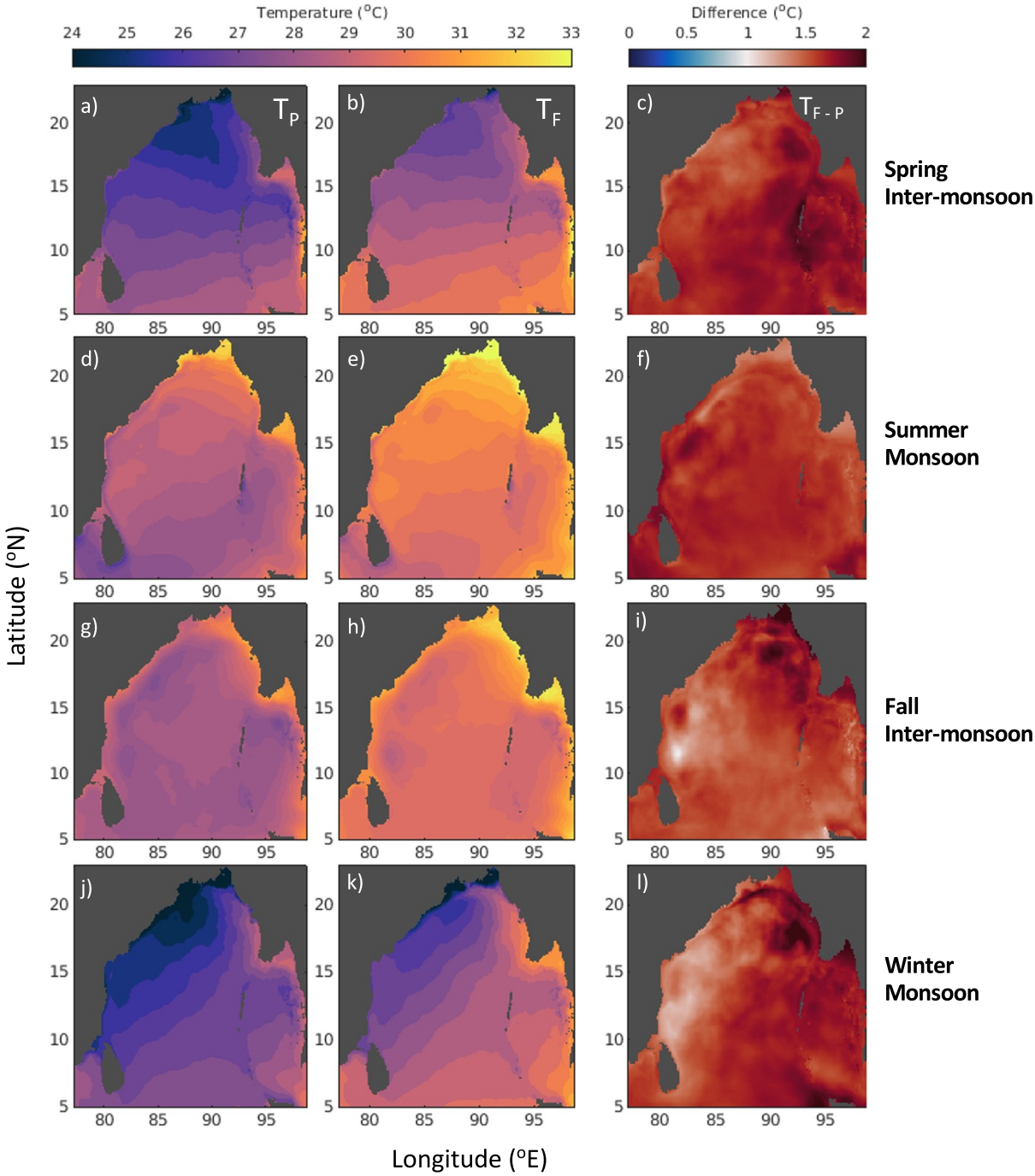

Figure 7. Surface (0–25 m) mean temperatures (°C) for the past (T_P; left column), future (T_F; middle column), and the difference between the future and past (T_{F-P}; right column), at 90% significance. Seasonal averages are denoted by the following rows: (a–c) spring (MAM); (d–f) summer (JJAS); (g–i) fall (ON); and (j–l) winter (DJF).

both fall and winter display a spatial discontinuity in T_{F-P}, with the western Bay of Bengal increasing by ~0.5–1°C less than the eastern Bay of Bengal.

Past to future changes in salinity (S_{F-P}) indicate the Bay of Bengal will become progressively fresher toward coastal regions in the north and eastern Bay of Bengal across all seasons (Figure 8). Significant freshening occurs in regions adjacent to shelves that receive large amounts of river runoff, such as from the Ganges and Irrawaddy rivers across all seasons, the southeastern region of the Bay of Bengal, and the southern Indian coast and Sri Lanka during fall and winter. Maximum S_{F-P} (−1.3 PSU) occurs off the coast of Myanmar during summer.

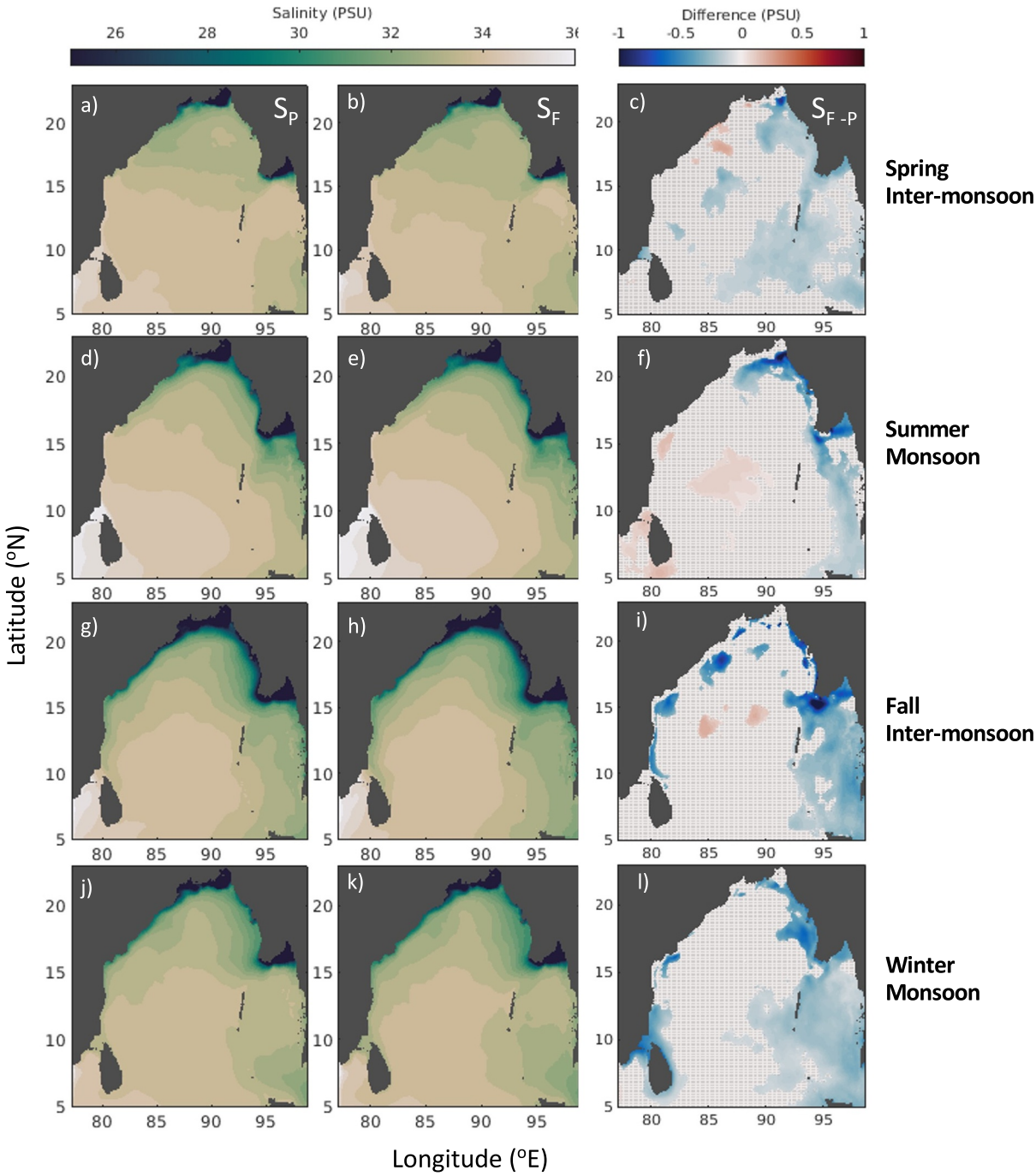

Figure 8. Surface (0–25 m) mean salinities (PSU) for the past (S_P; left column) and future (S_F; middle column), masked where not 90% significant between the future and past (S_{F-P}; right column). Seasonal averages are denoted by the following rows: (a–c) spring (MAM); (d–f) summer (JJAS); (g–i) fall (ON); and (j–l) winter (DJF).

Comparing the past and future precipitation rates (P_{F-P}) across the Bay of Bengal show seasonal differences in the distribution and intensity (Figure 9). Spring shows an overall reduction in precipitation over much of the region; however, isolated increases in P_{F-P} are centered across the Himalayas, the southern Bay of Bengal, and along 5°N. A similar distribution in P_{F-P} also occurs during the winter. Large increases in P_{F-P} of up to 2 m yr^{-1} occur during the summer across the north/northeast Bay of Bengal and across the Himalayas, consistent with previous studies (Dash et al., 2015) and with the CMIP6 ensemble (Katzenberger et al., 2021), and drives the elevated river runoff seen in Figure 10. Future river runoff in Region 1 (Myanmar coast) during August increases by 2532 km^3 yr^{-1}

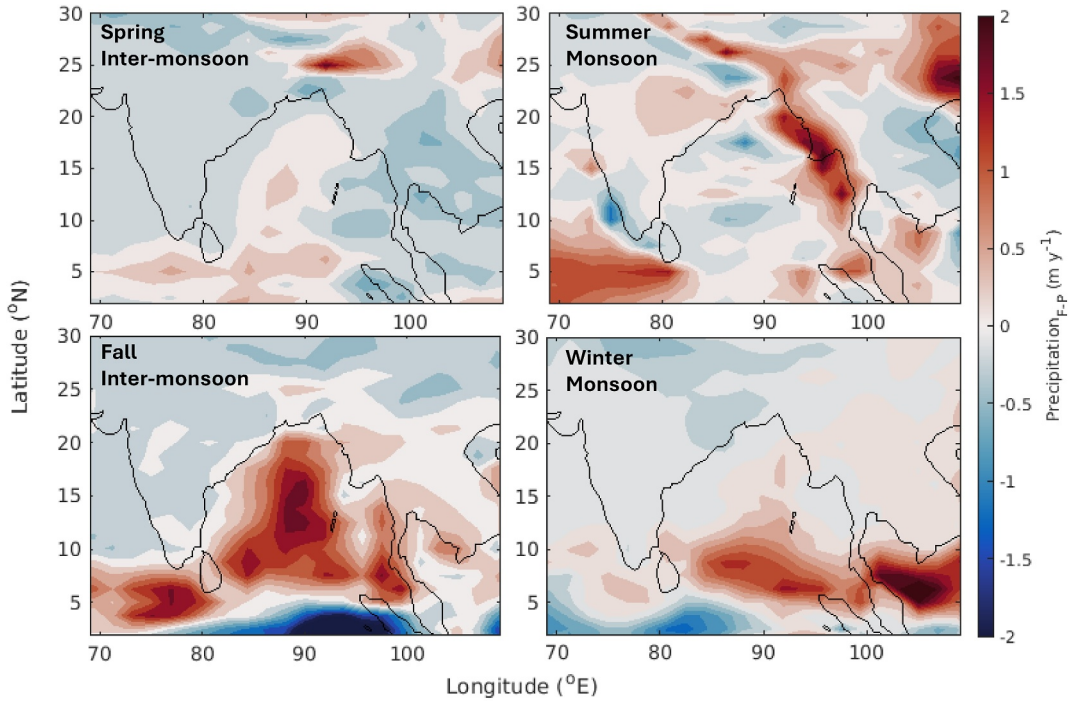

Figure 9. The difference in past and future precipitation (m yr^{-1}) across the Bay of Bengal region for spring, summer, fall, and winter from the driving HadGEM2 climate model.

more than Region 2 (head of Bay of Bengal), likely due to the distribution of precipitation over the respective river catchment areas during summer. During the fall, P_{F-P} increases in the Bay of Bengal's interior; however, this is not reflected in the salinity, which shows a small increase (Figure 8f) likely due to enhanced evaporation. Future precipitation rates decrease across the southern Indian subcontinent during summer and fall, and lead to a

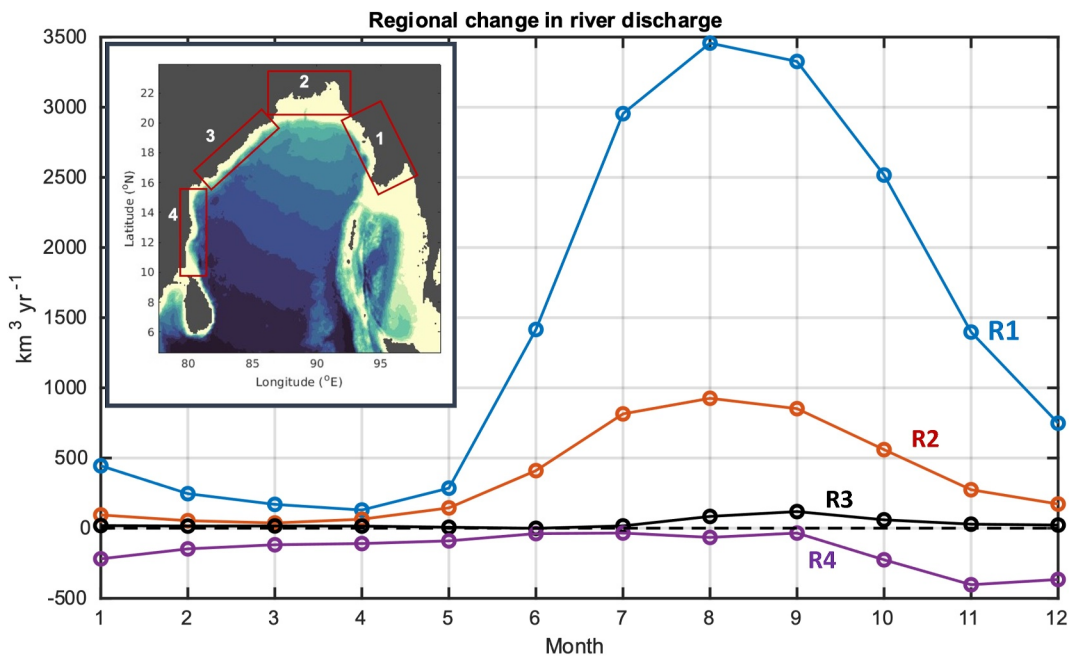

Figure 10. The total change in monthly river discharge (km^3 yr^{-1}) from past to future, for four regions around the Bay of Bengal, as identified by the red boxes in the inset map.

maximum reduction in river discharge of 403 $km^3\ yr^{-1}$ from the south of India (Region 4 in Figure 10). Regions of high river runoff (Regions 1 and 2 in Figure 10) have decreased concentrations of dissolved inorganic nitrate in the river water (Figure S10 in Supporting Information S1) because, in the GlobalNEWS2 model, the increase in river discharge exceeds the leaching rate of nitrate from the ground and dilutes the concentration of nitrate in the river water. Conversely, an increase in the dissolved inorganic nitrate concentration in river water occurs in Region 3 and Region 4 due to the regional reduction in future river runoff. However, the changes in river water nitrate concentrations are minor (Figure S10 in Supporting Information S1), and the impact in the ocean is constrained close to the coast.

Monthly wind speed differences from past to future ($Wind_{F-P}$) are highly variable but show an overall decrease in wind speeds across the Bay of Bengal and eastern Arabian Sea during the summer, but particularly in July and August (Figure S11 in Supporting Information S1). Further, toward fall, $Wind_{F-P}$ increases in the southern Bay of Bengal and reaches a maximum of change of +0.7 ms^{-1} during October. Crucially, these future intensified winds are still southwesterly and occur during the seasonal monsoon transition, as identified by the weak northeastern winds in the north of the Bay of Bengal. By November, wind direction is consistent across the Bay of Bengal but $Wind_{F-P}$ is still up to 2 ms^{-1} weaker.

Changes in $Wind_{F-P}$ drive circulation changes around the Bay of Bengal (Figure 11), and consequently the summer EICC also weakens by up to 0.08 ms^{-1} (identified by the black circle in Figure 11f). The opposite occurs during fall, with the coastal current along the southern India coast increasing by 0.4 m s^{-1} (identified in the black circle in Figure 11i) due to the enhanced southwesterly winds in October prolonging the SLD further into the fall. The resulting variability in surface currents during summer and fall–weaker in the north and stronger in the south–creates an asymmetric change in future circulation around the Bay of Bengal during the summer and postmonsoon season.

Significant future nitrate changes are predominantly positive across the Bay of Bengal with only small patches of negative change that occurs in the northeast Bay of Bengal during spring, in contrast to the global view that climate change will reduce surface nitrate concentrations (e.g., Hutchins & Fu, 2017). Increases in future nitrate concentrations (N_{F-P}; Figure 12) occur offshore from the Ganges and Irrawaddy shelves that correspond to regions of future freshening, suggesting the source of these elevated nitrate concentrations is the increased river runoff that travels further offshore. However, the reduction in future circulation around the northern Bay of Bengal during the summer (Figure 11i) acts to decrease the nitrate transports around the northern Bay of Bengal (Figure 13) by as much as 14.4%. The opposite occurs in the southern Bay of Bengal during fall, as the strong currents along the southern Indian coast result in an increased equatorward nitrate transport of up to 52%. This consequently leads to an increase in coastal nitrate concentrations (N_{F-P}) of 0.6 mmol N m^{-3} (Figure 12i) despite the reduction in local riverine runoff (Region 4 in Figure 10).

Future phytoplankton biomass is reduced on the Ganges shelf across all four seasons (Figure 14) and is likely due to the temperature response factor in ERSEM, which mimics the reduction of metabolic rates at higher temperatures (defined as a 32°-C ambient temperature threshold in ERSEM) due to enzyme degradation (Blackford et al., 2004; Butenschön et al., 2016)). As such, any increases in phytoplankton biomass in the northern Bay of Bengal become more restricted to areas where the temperature increases do not limit phytoplankton metabolic rates, such as shelf break regions and at the edges of riverine plumes. All phytoplankton groups show a reduction in biomass around the Indian coast between 12°N and 15°N during summer (Figures 15e–15h)). While there is no significant change in the nitrate concentrations in this region (Figure 12f), the small increase in salinity (Figure 8f) and the 11.5% decrease in nitrate transports during the summer (Figure 13) suggests less nutrient-rich river water is reaching this part of the Bay of Bengal due to the weakened circulation, limiting regional phytoplankton growth. Further offshore, the reduction in future phytoplankton biomass during summer could be due to increased surface temperatures, resulting in large areas exceeding the 32°-C temperature response threshold (Figure 7e) and thus reducing phytoplankton metabolic rates, as well as promoting more oligotrophic conditions through the intensification of stratification.

However, in the southern Bay of Bengal, localized diatom blooms occur along the southern Indian coastline during fall and winter (Figures 15i and 15m), corresponding to the increased nitrate concentrations (Figures 12i and 12l). Further offshore of Sri Lanka, all phytoplankton groups show an increase in biomass in the future during fall (Figures 15i–15l), which we attribute to upwelled nutrients from the SLD, as identified by the cooler surface temperatures in this region (Figure 7i).

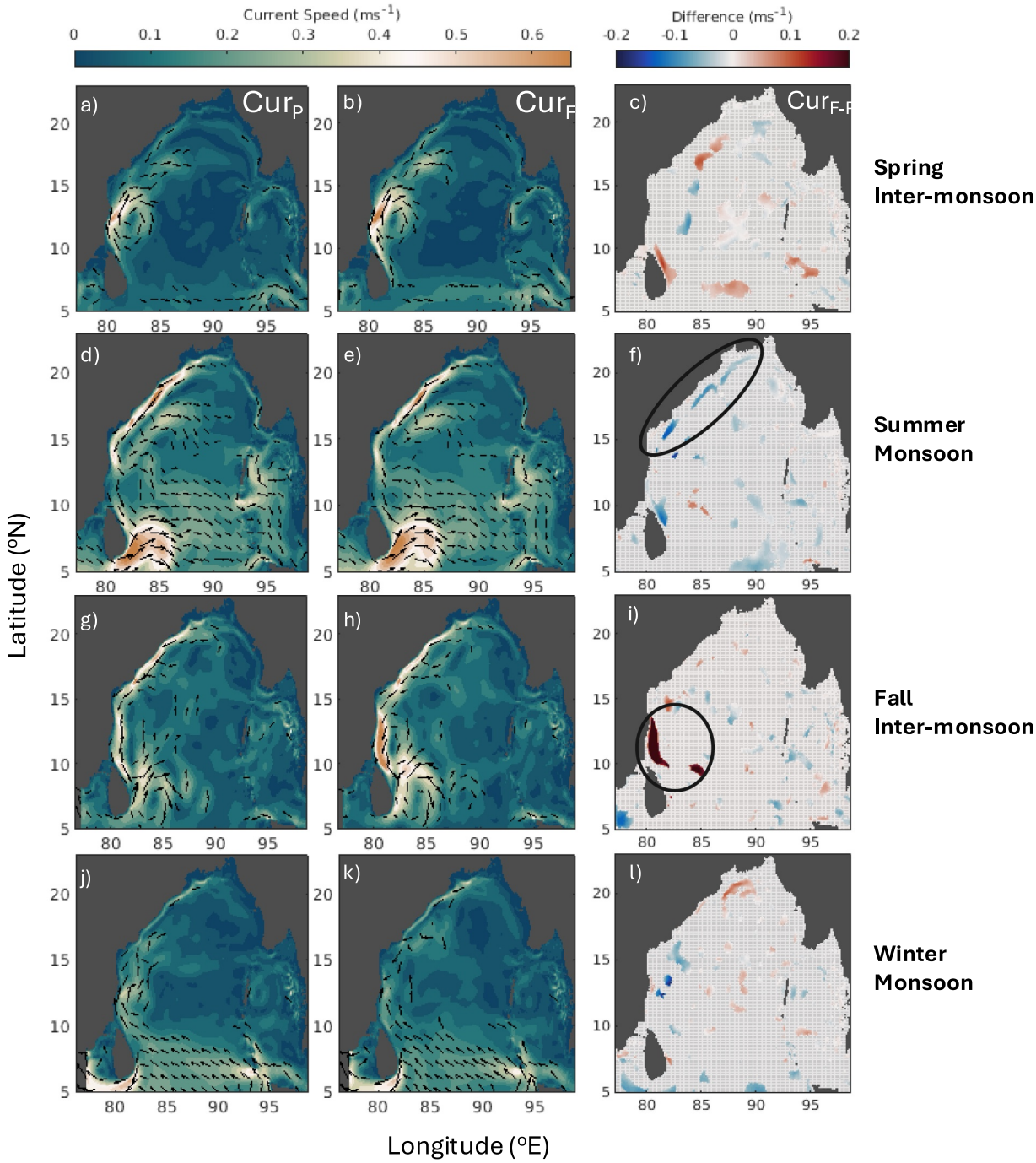

Figure 11. Surface (0–25 m) mean surface currents (ms^{-1}) for the past (Cur$_P$; left column), future (Cur$_F$; middle column), and the 90% significant difference between the future and past (Cur$_{F-P}$; right column). Seasonal averages are denoted by rows (a–c) spring (MAM); (d–f) summer (JJAS); (g–i) fall (ON); and (j–l) winter (DJF). The black loops indicate the main changes in the currents as discussed in the main text.

4. Discussion

4.1. Northern Bay of Bengal

From 1990 to 2060, our model showed a weakened circulation in the northern Bay of Bengal during summer, which limits phytoplankton growth further downstream despite the increase in river runoff. This rather

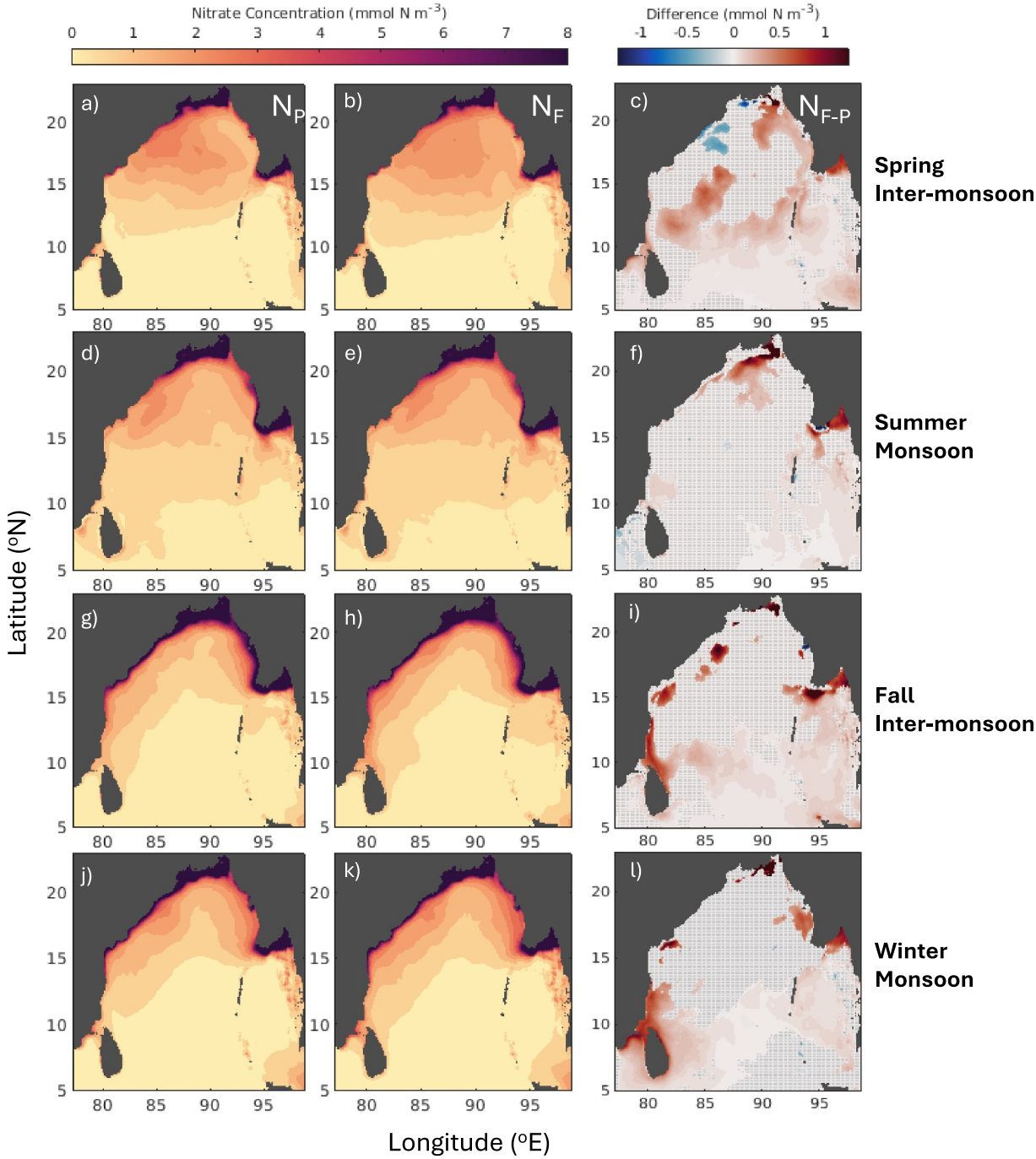

Figure 12. Surface (0–25 m) mean nitrate concentrations (mmol N m^{-3}) for the past (N_P; left column), future (N_F; middle column), and the 90% significant difference between the future and past (N_{F-P}; right column). Seasonal averages are denoted by rows (a–c) spring (MAM); (d–f) summer (JJAS); (g–i) fall (ON); and (j–l) winter (DJF).

counterintuitive view–nutrient limitation downstream despite higher river runoff–is supported by the reduction in future surface nitrate transport in the northern Bay of Bengal.

Reduced circulation in the northern Bay of Bengal due to wind, combined with the regionally positive P_{F-P}, can be attributed to the precipitation-wind paradox (Ueda et al., 2006). A reduction in wind speed would act to reduce the circulation in the northern Bay of Bengal, as seen in this study, and river runoff (from higher precipitation rates) would not be as efficiently transported out of the region. This leads to gradual surface freshening in the northern

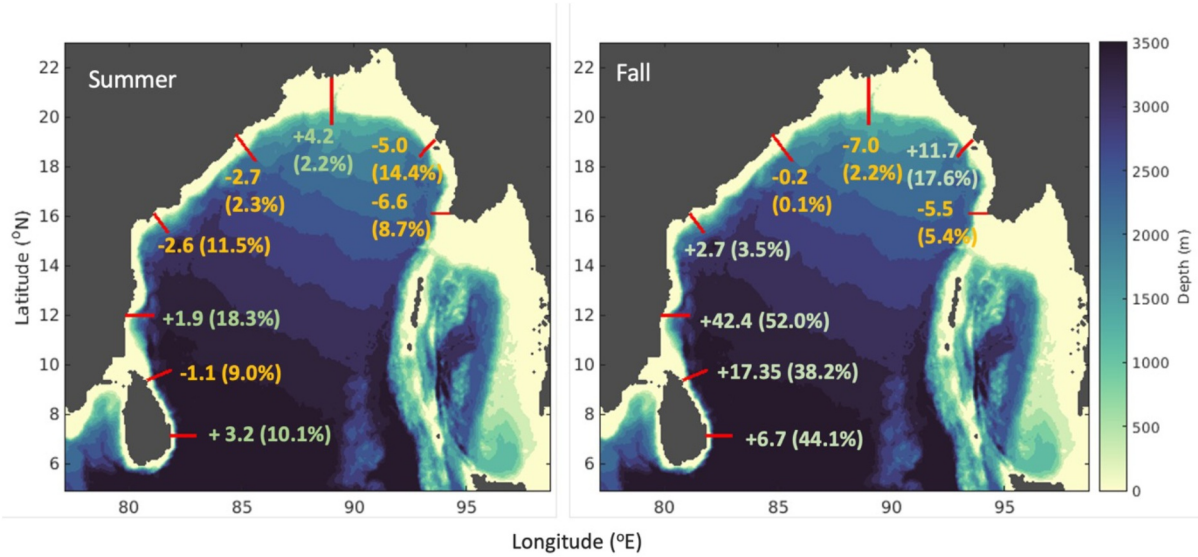

Figure 13. The change in total future nitrate transport (mmol N m^{-3} s^{-1}) across the red transect lines for summer (left) and fall (right), in an anticlockwise direction around the Bay of Bengal. Positive changes in nitrate transports are colored green and negative changes colored orange.

Bay of Bengal further offshore from the river source and a reduction in the horizontal density gradient across the Bay of Bengal, further suppressing density-driven coastal currents and propagating a positive feedback mechanism whereby the northern Bay of Bengal becomes progressively fresher during the summer and postmonsoon seasons. Combined with higher air temperatures, this leads to a future strengthening of surface stratification and perpetuates the oligotrophic conditions in the Bay of Bengal, supported by the overall reduction in phytoplankton biomass in the summer.

Intense stratification has already been shown to be a key factor in explaining why the Bay of Bengal is less productive than the Arabian Sea (Prasanna Kumar et al., 2002) as it creates a barrier to nutrients being fluxed to the surface. Although tropical cyclones are not resolved in the CMIP models (Le Guenedal et al., 2022), it can be assumed that in the future, increasing surface temperatures in the Bay of Bengal would strengthen stratification and consequently, stronger cyclones, like those predicted to occur across the region (Balaguru et al., 2014), will become an increasingly important mechanism to erode the stratified layer and promote diapycnal nitrate fluxes. However, given the added freshwater stratification from increased future river runoff, even the most extreme cyclones may not be energetic enough to promote mixing, especially during periods of heavy rainfall (Maneesha et al., 2011), which would hinder the essential replenishment of limiting nutrients and sustain widespread oligotrophic conditions in the Bay of Bengal.

In reality, it can be assumed that the reduction in future phytoplankton biomass seen in this study is underestimated due to the increased amounts of suspended particulate matter (not included in this model) that would be delivered to coastal regions with the river runoff (e.g., Ittekkot et al., 1991; Masud-Ul-Alam et al., 2021; Michels et al., 2003), as this would inhibit near-coastal primary productivity through light limitation (Bharathu et al., 2018) and could further exacerbate the pressure on the fishing industry, risking livelihoods and food security. Warming surface temperatures would also directly impact the production rate of key fish species, such as Hilsa (*Tenualosa ilisha*)—a migratory fish where 90% of the global catch is from Bangladesh, India, and Myanmar—whose migratory life cycle is highly dependent on temperature (Jahan et al., 2017). Das et al. (2020) further showed that increased temperatures in the Bay of Bengal, as shown in this study, would reduce the fisheries industries by 5%, leading to an economic loss of 1.7 billion USD by 2050.

4.2. Southern Bay of Bengal

In contrast to the northern Bay of Bengal, the southern Bay of Bengal displayed elevated surface currents along the southeast Indian coast, increasing equatorward nitrate transport. This current intensification can be attributed to increases in local wind stress during the fall, corroborated by our analysis and from previous observations

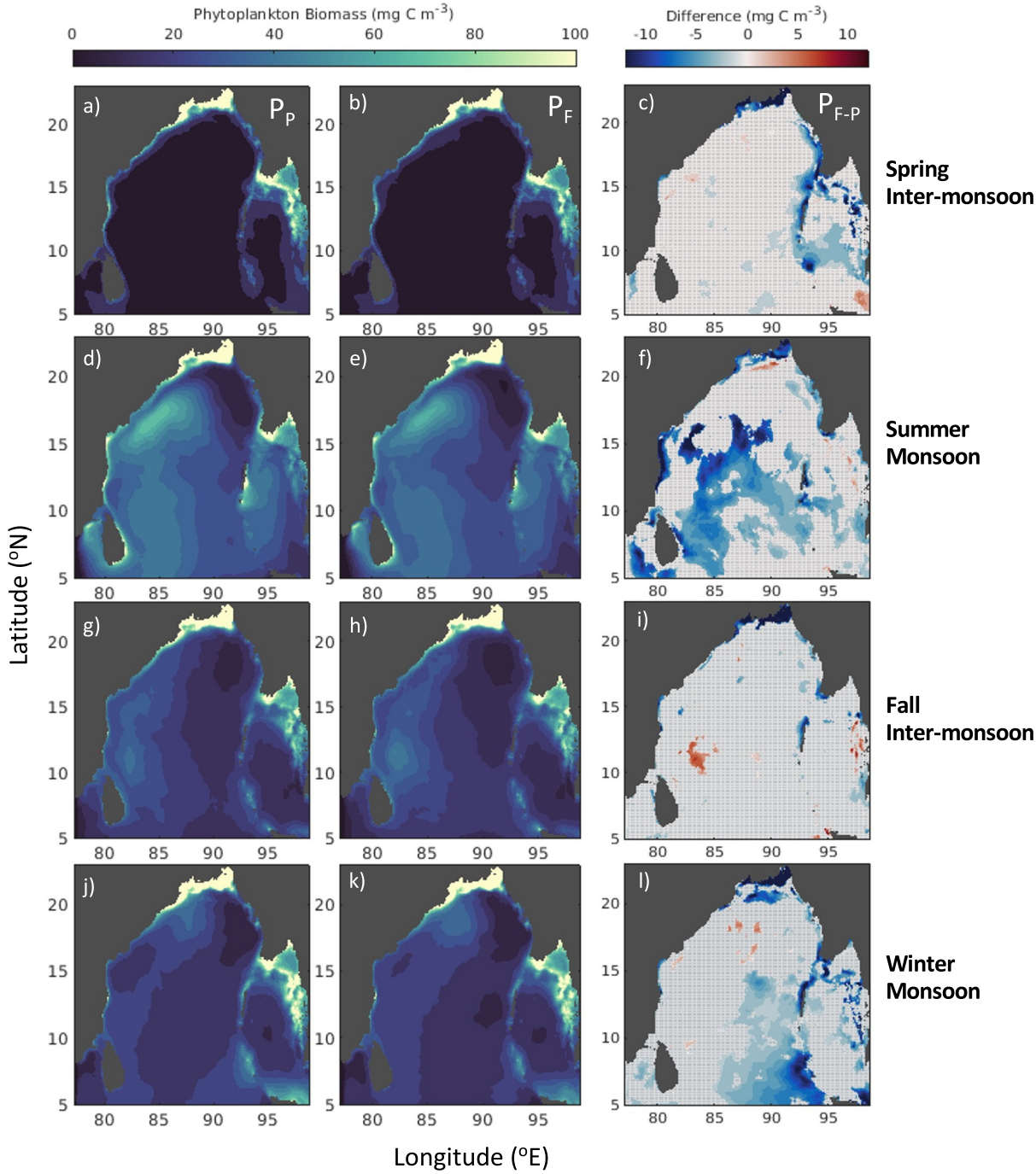

Figure 14. Surface (0–25 m) mean concentration of phytoplankton biomass (mg C m^{-3}) for the past (Ph_P; left column), future (Ph_F; middle column), and the 90% significant difference between the future and past (Ph_{F-P}; right column). Seasonal averages are denoted by rows (a–c) spring (MAM); (d–f) summer (JJAS); (g–i) fall (ON); and (j–l) winter (DJF).

(Joseph & Simon, 2005), that sustain the SLD further into the season. A predicted delayed retreat to the summer monsoon, combined with the elevated wind speeds around southern India, would also explain why the SLD is sustained further into the fall in this study.

The longevity of the SLD–existing well into the postmonsoon season, rather than dissipating during late summer–prolongs nutrient transport around the region. Surface currents associated with the SLD more efficiently facilitate the equatorward transport of riverine nutrients, especially from the east Indian rivers such as the Krishna and

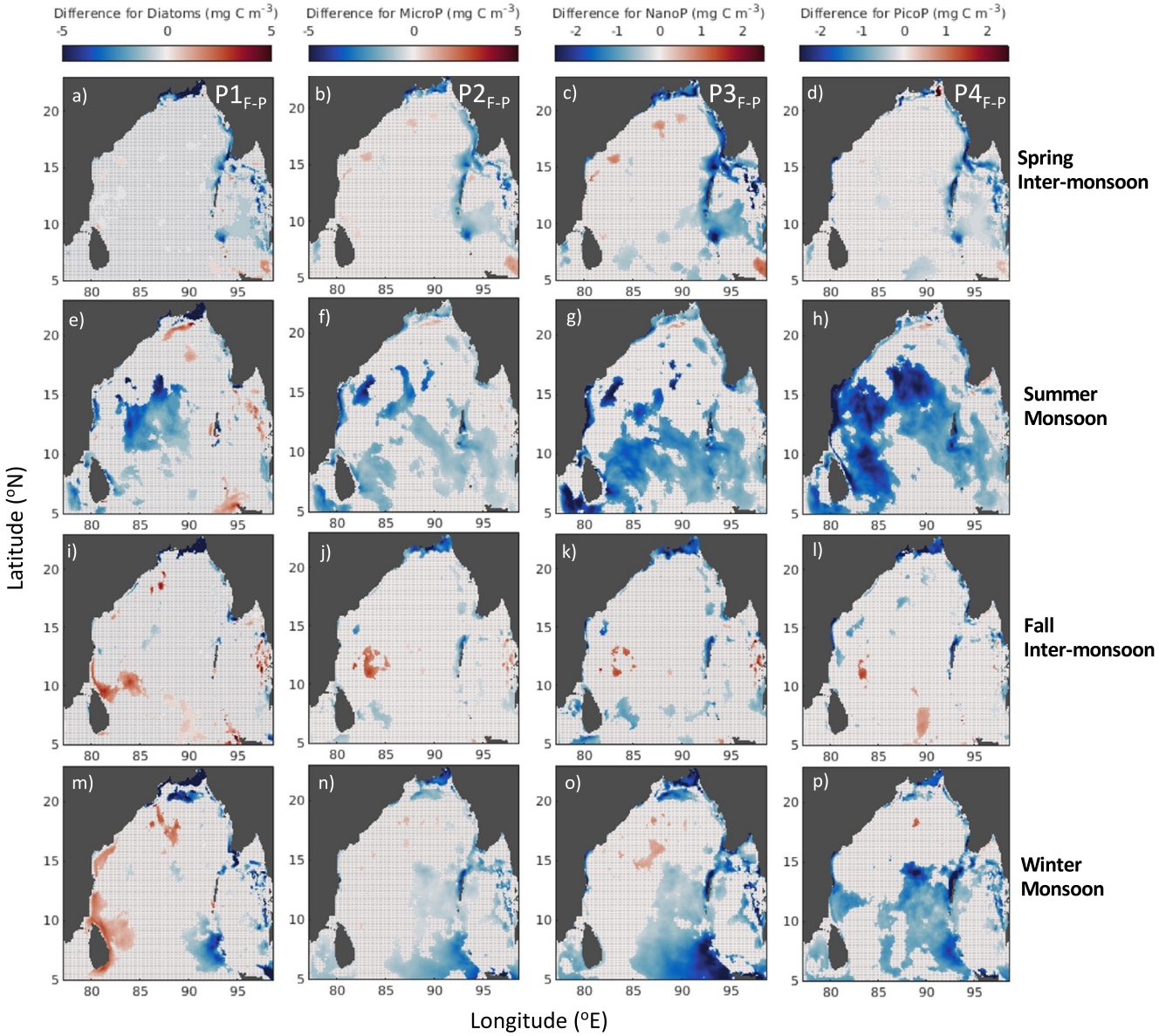

Figure 15. Surface (0–25 m) mean difference in past and future phytoplankton biomass (mg C m^{-3}) for diatoms ($P1_{F-P}$; left column), microphytoplankton ($P2_{F-P}$); picophytoplankton ($P3_{F-P}$), and nanophytoplankton ($P4_{F-P}$), at 90% confidence. Seasonal averages are denoted by rows (a–c) spring (MAM); (d–f) summer (JJAS); (g–i) fall (ON); and (j–l) winter (DJF).

Godavari (Region 3 in Figure 10). This response is offset slightly by the predicted reduction in runoff in southern India (Region 4 in Figure 10), but while river runoff in Region 4 did show some elevated nitrate concentrations, the substantial increase in future nitrate transport suggests changes in circulation are more important for nutrient distribution around the Bay of Bengal than the predicted changes in river runoff.

An extended summer monsoon–and by extension the Summer Monsoon Current–is predicted to alter the phytoplankton community structure and enhance the biogenic carbon flux in the southern Bay of Bengal (Jyothibabu et al., 2015), partly through elevated riverine nutrients promoting diatom blooms along the southern Indian coast. Diatoms are the preferential food source of certain fish species in the Bay of Bengal (Dutta et al., 2014), implying these future blooms would be advantageous for local fishing communities. However, excess nutrients transported into the region would also negatively impact the ecosystem through more frequent eutrophication events and harmful algal blooms (e.g., Chakrabarti & Ray, 2017; Khan et al., 2019;

Thirumalaiselvan et al., 2023). Not only would this increase the health risk to coastal communities, but this would also be economically damaging to coastal regions that heavily rely on tourism (e.g., Fonseca et al., 2021).

Further offshore, the intensified SLD further supports phytoplankton growth via the upwelling of nutrients from the deep ocean (Thushara et al., 2019). Elevated nitrate transports around the southern tip of India would promote localized phytoplankton blooms in the southern Arabian Sea (Prasanna Kumar et al., 2004). However, this could also lead to more eutrophication events, especially along the west Indian coast. Future work will explore how the ecosystem along the west coast of India responds to future EICC/SLD variability.

4.3. Model Uncertainties

Uncertainties from the ROAM model leads to biases in the SEAsia Climate model. However, providing a quantitative assessment and predictions of the future changes within a space of uncertainty would require an ensemble of projections driven by different scenarios, different atmospheric/large ocean conditions (i.e., from different CMIP models), and different runoff scenarios. Instead, this study includes process parameterizations that require the model to be run with a time step and resolution that is very computationally expensive, meaning only one projection is feasible. Nevertheless, this study aims to inform about processes and system mechanics from changes in circulation and rainfall-runoffs in the Bay of Bengal, and uncertainties through bias in the model results have been reduced by only including the F–P changes at 90% significance.

The Bay of Bengal region in the SEAsia model is highly influenced by the boundary conditions enforced from the ROAM model along the 77°E longitudinal line. Variations in the position and intensity of the Summer Monsoon Current would be influenced by biases arising from these boundary conditions, which could further influence the position of the SLD. While the 1/12th-degree resolution of the model greatly improves upon the coarser 1/4th-degree resolution of ROAM, errors could still arise from the representation of subgrid scale processes, especially those resulting from biological processes and are by definition highly patchy. Sea surface temperature and salinity biases from SEAsia Hindcast (Figures 2a, 2d, 3a, and 3d) are within acceptable limits and show skill in the model when using realistic atmospheric forcing (ERA5). However, unlike ERA5, the atmospheric model used for forcing in SEAsia Climate is not constrained to observations. Extrapolating the biases in the SEAsia Climate run in the past and future time periods is not feasible as it depends on the properties of the HadGEM forcing as on the response of the NEMO ocean model. Furthermore, we chose against incorporating a bias correction in order for key processes to evolve freely within the model.

The choice of river model is another source of uncertainty as our model did not assume the extra runoff from melting glaciers, changing land or fertilizer use, or any changes in hydrology (e.g., new dams, reservoirs etc.); it can be assumed that both runoff magnitude and riverine nitrate concentrations might be higher in reality than shown in this study, further exacerbating future ecosystem changes. Largest uncertainties arise from the choice of the climate model used to force the SEAsia Climate model, and while no model is an exact replica of reality, we have shown through extensive validation that errors resulting from biases in the forcing models are limited in the present day model results.

5. Conclusions

This study aims to understand how circulation and nitrate transport in the Bay of Bengal could change under a potential future climate change scenario. Using a coupled physics-ecosystem model, future changes in temperature, salinity, nitrate concentrations, nitrate transport, current speeds, and phytoplankton biomass were studied from 1980 to 2060 under an RCP8.5 emissions scenario (SEAsia Climate). Across two contrasting time periods (1990–2010 and 2040–2060), the model predicted a reduced circulation in the northern Bay of Bengal and accelerated coastal currents along southern India. We suggest this is from a weaker and longer summer monsoon, as highlighted by the reduced wind speeds across the Bay of Bengal during summer and intensified winds in the southeast Bay of Bengal during fall.

Despite the asymmetric changes in circulation being highly localized changes, they have far-reaching effects on the nutrient transports around the Bay of Bengal. For example, the northern Bay of Bengal displays a stark decrease in nitrate transports in the future, despite the higher riverine runoff, leading to a gradual freshening in the north/northeast Bay of Bengal. Conversely, the southern Bay of Bengal displayed greatly elevated equatorward

nitrate transports despite the decrease in precipitation and river runoff across southern India, resulting in localized diatom blooms along the Indian coast.

In this study, we not only highlight the vulnerability of the Bay of Bengal of Bengal to a changing climate, but emphasize the importance of a detailed regional view of climate change, particularly in areas where future changes in most parameters (except temperature) are dependent on the complex interplay of regional processes.

Conflict of Interest

The authors declare no conflicts of interest relevant to this study.

Data Availability Statement

The model data used in this study (a subset of the SEAsia model) can be found in the public Jasmin repository here: https://gws-access.jasmin.ac.uk/public/accord/ACCORD_SEAsia. The data used for the model validation were downloaded from the World Ocean Atlas Database 2023, accessed here: https://www.ncei.noaa.gov/products/world-ocean-database. Sea surface temperature satellite data are the Level 4 SST CCI analysis product, and can be downloaded from the CEDA archive here: https://catalogue.ceda.ac.uk/uuid/debfbf49823f4eb99ab0a578f8b25136. Satellite chlorophyll data used for validation are the merged data set and was downloaded from the Ocean Colour Climate Change Initiative, European Space Agency, available online at http://www.esa-oceancolour-cci.org. OSCAR current data used for validation are available here: https://podaac.jpl.nasa.gov/dataset/OSCAR_L4_OC_FINAL_V2.0.

Acknowledgments
This research was funded through NERC, in conjunction with the National Oceanography Centre and the Plymouth Marine Laboratory, as part of the Future States of the Global Coastal Ocean (FOCUS) project (NE/X006271/1), as well as the UKRI-GCRF funded project South Asian Nitrogen Hub (SANH; NE/S009019/).

References

Amol, P., Vinayachandran, P. N., Shankar, D., Thushara, V., Vijith, V., Chatterjee, A., & Kankonkar, A. (2020). Effect of freshwater advection and winds on the vertical structure of chlorophyll in the northern Bay of Bengal. *Deep Sea Research Part II: Topical Studies in Oceanography*, *179*, 104622. https://doi.org/10.1016/j.dsr2.2019.07.010

Balaguru, K., Taraphdar, S., Leung, L. R., & Foltz, G. R. (2014). Increase in the intensity of postmonsoon Bay of Bengal tropical cyclones. *Geophysical Research Letters*, *41*(10), 3594–3601. https://doi.org/10.1002/2014gl060197

Baretta, J. W., Ebenhöh, W., & Ruardij, P. (1995). The European regional seas ecosystem model, a complex marine ecosystem model. *Netherlands Journal of Sea Research*, *33*(3–4), 233–246. https://doi.org/10.1016/0077-7579(95)90047-0

Beusen, A. H. W., Bouwman, A. F., Dürr, H. H., Dekkers, A. L. M., & Hartmann, J. (2009). Global patterns of dissolved silica export to the coastal zone: Results from a spatially explicit global model. *Global Biogeochemical Cycles*, *23*(4). https://doi.org/10.1029/2008gb003281

Bharathi, M. D., Sarma, V. V. S. S., Ramaneswari, K., & Venkataramana, V. (2018). Influence of river discharge on abundance and composition of phytoplankton in the western coastal Bay of Bengal during peak discharge period. *Marine Pollution Bulletin*, *133*, 671–683. https://doi.org/10.1016/j.marpolbul.2018.06.032

Blackford, J. C., Allen, J. I., & Gilbert, F. J. (2004). Ecosystem dynamics at six contrasting sites: A generic modelling study. *Journal of Marine Systems*, *52*(1–4), 191–215. https://doi.org/10.1016/j.jmarsys.2004.02.004

Bricker, S. B., Longstaff, B., Dennison, W., Jones, A., Boicourt, K., Wicks, C., & Woerner, J. (2008). Effects of nutrient enrichment in the nation's estuaries: A decade of change. *Harmful Algae*, *8*(1), 21–32. https://doi.org/10.1016/j.hal.2008.08.028

Bruggeman, J., & Bolding, K. (2014). A general framework for aquatic biogeochemical models. *Environmental Modelling & Software*, *61*, 249–265. https://doi.org/10.1016/j.envsoft.2014.04.002

Butenschön, M., Clark, J., Aldridge, J. N., Allen, J. I., Artioli, Y., Blackford, J., et al. (2016). Ersem 15.06: A generic model for marine biogeochemistry and the ecosystem dynamics of the lower trophic levels. *Geoscientific Model Development*, *9*(4), 1293–1339. https://doi.org/10.5194/gmd-9-1293-2016

Canuto, V. M., Howard, A., Cheng, Y., & Dubovikov, M. S. (2001). Ocean turbulence. Part I: One-Point closure model—Momentum and heat vertical diffusivities. *Journal of Physical Oceanography*, *31*(6), 1413–1426. https://doi.org/10.1175/1520-0485(2001)031<1413:OTPIOP>2.0.CO;2

Chakrabarti, S., & Ray, R. (2017). Coastal eutrophication as a cause of elimination of lugworms: First record of Arenicola marina (Linnaeus, 1758) from coastal areas of Bay of Bengal at Chandipur, Odisha, India. *World Scientific News*, *71*, 22–27.

Chatterjee, A., Dutta, C., Jana, T. K., & Sen, S. (2012). Fine mode aerosol chemistry over a tropical urban atmosphere: Characterization of ionic and carbonaceous species. *Journal of Atmospheric Chemistry*, *69*(2), 83–100. https://doi.org/10.1007/s10874-012-9231-8

Cullen, K. E., & Shroyer, E. L. (2019). Seasonality and interannual variability of the Sri Lanka dome. *Deep Sea Research Part II: Topical Studies in Oceanography*, *168*, 104642. https://doi.org/10.1016/j.dsr2.2019.104642

Das, I., Lauria, V., Kay, S., Cazcarro, I., Arto, I., Fernandes, J. A., & Hazra, S. (2020). Effects of climate change and management policies on marine fisheries productivity in the North-East coast of India. *Science of the Total Environment*, *724*, 138082. https://doi.org/10.1016/j.scitotenv.2020.138082

Dash, S. K., Mishra, S. K., Pattnayak, K. C., Mamgain, A., Mariotti, L., Coppola, E., et al. (2015). Projected seasonal mean summer monsoon over India and adjoining regions for the twenty-first century. *Theoretical and Applied Climatology*, *122*(3–4), 581–593. https://doi.org/10.1007/s00704-014-1310-0

De Vos, A., Pattiaratchi, C. B., & Wijeratne, E. M. S. (2014). Surface circulation and upwelling patterns around Sri Lanka. *Biogeosciences*, *11*(20), 5909–5930. https://doi.org/10.5194/bg-11-5909-2014

DRAKKAR Group. (2007). Eddy-permitting ocean circulation hindcasts of past decades (Technical report). *CLIVAR-Exchanges*, *12*(3), 8–10.

Drenkard, E. J., Stock, C., Ross, A. C., Dixon, K. W., Adcroft, A., Alexander, M., et al. (2021). Next-generation regional ocean projections for living marine resource management in a changing climate. *ICES Journal of Marine Science*, *78*(6), 1969–1987. https://doi.org/10.1093/icesjms/fsab100

Dutta, S., Maity, S., Bhattacharyya, S. B., Sundaray, J. K., & Hazra, S. (2014). Diet composition and intensity of feeding of Tenualosa Ilisha (Hamilton, 1822) occurring in the northern Bay of Bengal, India. In *Proceedings of the zoological society*, (Vol. 67(1), pp. 33–37). Springer. https://doi.org/10.1007/s12595-013-0066-3

Embury, O., Good, S. A., Alerskans, E., & Høyer, J. L. (2024). ESA sea surface temperature climate change Initiative (SST_cci): Climate data record version 3.0 [Dataset: Level 4 SST CCI analysis product]. *NERC EDS Centre for Environmental Data Analysis*. http://catalogue.ceda.ac.uk/uuid/debfbf49823f4eb99ab0a578f8b25136/

ESR, Dohan, & Kathleen. (2022). Ocean surface current Analyses Real-time (OSCAR) surface currents—Final 0.25 degree (version 2.0). Ver. 2.0. [Dataset]. *PO.DAAC*. [Dataset: OSCAR satellite data]. https://doi.org/10.5067/OSCAR-25F20

Flather, R. A. (1994). A storm surge prediction model for the northern Bay of Bengal with application to the cyclone disaster in April 1991. *Journal of Physical Oceanography*, *24*(1), 172–190. https://doi.org/10.1175/1520-0485(1994)024<0172:ASSPMF>2.0.CO;2

Fonseca, A. L., Newton, A., & Cabral, A. (2021). Local and Meso-scale pressures in the eutrophication process of a coastal subtropical system: Challenges for effective management. *Estuarine, Coastal and Shelf Science*, *250*, 107109. https://doi.org/10.1016/j.ecss.2020.107109

Gill, A. E. (1982). *Atmosphere-ocean dynamics* (Vol. 30). Academic Press.

Girishkumar, M. S., Ravichandran, M., McPhaden, M. J., & Rao, R. R. (2011). Intraseasonal variability in barrier layer thickness in the south central Bay of Bengal. *Journal of Geophysical Research*, *116*(C3), C03009. https://doi.org/10.1029/2010jc006657

Gomes, H. R., Goes, J. I., & Saino, T. (2000). Influence of physical processes and freshwater discharge on the seasonality of phytoplankton regime in the Bay of Bengal. *Continental Shelf Research*, *20*(3), 313–330. https://doi.org/10.1016/s0278-4343(99)00072-2

Goswami, B. N., Chakraborty, D., Rajesh, P. V., & Mitra, A. (2022). Predictability of south-Asian monsoon rainfall beyond the legacy of Tropical Ocean Global Atmosphere program (TOGA). *npj Climate and Atmospheric Science*, *5*(1), 58. https://doi.org/10.1038/s41612-022-00281-3

Ha, K. J., Moon, S., Timmermann, A., & Kim, D. (2020). Future changes of summer monsoon characteristics and evaporative demand over Asia in CMIP6 simulations. *Geophysical Research Letters*, *47*(8), e2020GL087492. https://doi.org/10.1029/2020gl087492

Han, W., McCreary, J. P., Jr., & Kohler, K. E. (2001). Influence of precipitation minus evaporation and Bay of Bengal rivers on dynamics, thermodynamics, and mixed layer physics in the upper Indian Ocean. *Journal of Geophysical Research*, *106*(C4), 6895–6916. https://doi.org/10.1029/2000jc000403

Hutchins, D. A., & Fu, F. (2017). Microorganisms and ocean global change. *Nature microbiology*, *2*(6), 1–11. https://doi.org/10.1038/nmicrobiol.2017.58

Islam, M. L., Alam, M. J., Rheman, S., Ahmed, S. U., & Mazid, M. A. (2004). Water quality, nutrient dynamics and sediment profile in shrimp farms of the Sundarbans mangrove forest, Bangladesh. Retrieved from http://nopr.niscpr.res.in/handle/123456789/1663

Ittekkot, V., Nair, R. R., Honjo, S., Ramaswamy, V., Bartsch, M., Manganini, S., & Desai, B. N. (1991). Enhanced particle fluxes in Bay of Bengal induced by injection of fresh water. *Nature*, *351*(6325), 385–387. https://doi.org/10.1038/351385a0

Jahan, I., Ahsan, D., & Farque, M. H. (2017). Fishers' local knowledge on impact of climate change and anthropogenic interferences on Hilsa fishery in South Asia: Evidence from Bangladesh. *Environment, Development and Sustainability*, *19*(2), 461–478. https://doi.org/10.1007/s10668-015-9740-0

Joseph, P. V., & Simon, A. (2005). Weakening trend of the southwest monsoon current through peninsular India from 1950 to the present. *Current Science*, 687–694.

Jyothibabu, R., Vinayachandran, P. N., Madhu, N. V., Robin, R. S., Karnan, C., Jagadeesan, L., & Anjusha, A. (2015). Phytoplankton size structure in the southern Bay of Bengal modified by the Summer Monsoon Current and associated eddies: Implications on the vertical biogenic flux. *Journal of Marine Systems*, *143*, 98–119. https://doi.org/10.1016/j.jmarsys.2014.10.018

Katavouta, A., Polton, J. A., Harle, J. D., & Holt, J. T. (2022). Effect of tides on the Indonesian seas circulation and their role on the volume, heat and salt transports of the Indonesian throughflow. *Journal of Geophysical Research: Oceans*, *127*(8), e2022JC018524. https://doi.org/10.1029/2022jc018524

Katzenberger, A., Schewe, J., Pongratz, J., & Levermann, A. (2021). Robust increase of Indian monsoon rainfall and its variability under future warming in CMIP6 models. *Earth System Dynamics*, *12*(2), 367–386. https://doi.org/10.5194/esd-12-367-2021

Khan, S., Jahan, R., Rahman, M. A., & Haque, M. M. (2019). Eutrophication enhances phytoplankton abundance in the Maheshkhali channel, Bay of Bengal, Bangladesh. *Aust. J. Sci. Techno*, *3*, 141–147.

Krishna, M. S., Prasad, M. H. K., Rao, D. B., Viswanadham, R., Sarma, V. V. S. S., & Reddy, N. P. C. (2016). Export of dissolved inorganic nutrients to the northern Indian Ocean from the Indian monsoonal rivers during discharge period. *Geochimica et Cosmochimica Acta*, *172*, 430–443. https://doi.org/10.1016/j.gca.2015.10.013

Kumar, B. S. K., Bhaskararao, D., Krishna, P., Lakshmi, C. N., Surendra, T., & Krishna, R. M. (2022). Impact of nutrient concentration and composition on shifting of phytoplankton community in the coastal waters of the Bay of Bengal. *Regional Studies in Marine Science*, *51*, 102228. https://doi.org/10.1016/j.rsma.2022.102228

Kuttippurath, J., Sunanda, N., Martin, M. V., & Chakraborty, K. (2021). Tropical storms trigger phytoplankton blooms in the deserts of north Indian Ocean. *NPJ Climate and Atmospheric Science*, *4*(1), 11. https://doi.org/10.1038/s41612-021-00166-x

Le Guenedal, T., Drobinski, P., & Tankov, P. (2022). Cyclone generation algorithm including a THERmodynamic module for Integrated National damage assessment (CATHERINA 1.0) compatible with Coupled Model Intercomparison Project (CMIP) climate data. *Geoscientific Model Development*, *15*(21), 8001–8039. https://doi.org/10.5194/gmd-15-8001-2022

Levier, B., Tréguier, A.-M., Madec, G., & Garnier, V. (2007). Free surface and variable volume in the nemo code. (Tech. Rep.). https://doi.org/10.5281/zenodo.3244182

Luneva, M. V., Aksenov, Y., Harle, J. D., & Holt, J. T. (2015). The effects of tides on the water mass mixing and sea ice in the Arctic Ocean. *Journal of Geophysical Research: Oceans*, *120*(10), 6669–6699. https://doi.org/10.1002/2014jc010310

Lyard, F. H., Allain, D. J., Cancet, M., Carrère, L., & Picot, N. (2021). FES2014 global ocean tide atlas: Design and performance. *Ocean Science*, *17*(3), 615–649. https://doi.org/10.5194/os-17-615-2021

Ma, J., & Yu, J. Y. (2014). Paradox in South Asian summer monsoon circulation change: Lower tropospheric strengthening and upper tropospheric weakening. *Geophysical Research Letters*, *41*(8), 2934–2940. https://doi.org/10.1002/2014gl059891

Madec, G., Bourdallé-Badie, R., Bouttier, P. A., Bricaud, C., Bruciaferri, D., Calvert, D., et al. (2017). NEMO ocean engine.

Maneesha, K., Sarma, V. V. S. S., Reddy, N. P. C., Sadhuram, Y., Murty, T. R., Sarma, V. V., & Kumar, M. D. (2011). Meso-scale atmospheric events promote phytoplankton blooms in the coastal Bay of Bengal. *Journal of Earth System Science*, *120*(4), 773–782. https://doi.org/10.1007/s12040-011-0089-y

Masud-Ul-Alam, M., Khan, M. A. I., Islam, M. N., & Rahman, S. M. (2021). Modeling spatio-temporal variability of suspended matter and its relation with hydrodynamic parameters in the northern Bay of Bengal. *Modeling Earth Systems and Environment*, *7*(4), 2517–2530. https://doi.org/10.1007/s40808-020-01053-9

Mayorga, E., Seitzinger, S. P., Harrison, J. A., Dumont, E., Beusen, A. H., Bouwman, A. F., et al. (2010). Global Nutrient Export from WaterSheds 2 (NEWS 2): Model development and implementation. *Environmental Modelling and Software*, *25*(7), 837–853. https://doi.org/10.1016/j.envsoft.2010.01.007

Michels, K. H., Suckow, A., Breitzke, M., Kudrass, H. R., & Kottke, B. (2003). Sediment transport in the shelf canyon "swatch of No ground"(bay of Bengal). *Deep Sea Research Part II: Topical Studies in Oceanography*, *50*(5), 1003–1022. https://doi.org/10.1016/s0967-0645(02)00617-3

Mishonov, A. V., Boyer, T. P., Baranova, O. K., Bouchard, C. N., Garcia, S. C. H. E., Locarnini, R. A., et al. (2024). World Ocean Database 2023. In C. Bouchard (Ed.), *NOAA Atlas NESDIS*, (Vol. *97*, p. 206). https://doi.org/10.25923/z885-h264

Mishra, R. K., Shaw, B. P., Sahu, B. K., Mishra, S., & Senga, Y. (2009). Seasonal appearance of chlorophyceae phytoplankton bloom by river discharge off Paradeep at Orissa coast in the Bay of Bengal. *Environmental Monitoring and Assessment*, *149*(1–4), 261–273. https://doi.org/10.1007/s10661-008-0200-2

Naik, R. K., Hegde, S., & Anil, A. C. (2011). Dinoflagellate community structure from the stratified environment of the Bay of Bengal, with special emphasis on harmful algal bloom species. *Environmental Monitoring and Assessment*, *182*(1–4), 15–30. https://doi.org/10.1007/s10661-010-1855-z

Partridge, D. (2022). Dalepartridge/ACCORD_SEAsia_BGCsetup: ACCORD NEMO-FABM setup for ERSEM Biogeochemistry (v1.0.0). *Zenodo*. https://doi.org/10.5281/zenodo.6940833

Potemra, J. T., Luther, M. E., & O'Brien, J. J. (1991). The seasonal circulation of the upper ocean in the Bay of Bengal. *Journal of Geophysical Research*, *96*(C7), 12667–12683. https://doi.org/10.1029/91jc01045

Prasad, T. G. (1997). Annual and seasonal mean buoyancy fluxes for the tropical Indian Ocean. *Current Science*, 667–674.

Prasanna Kumar, S., Muraleedharan, P. M., Prasad, T. G., Gauns, M., Ramaiah, N., De Souza, S. N., et al. (2002). Why is the Bay of Bengal less productive during summer monsoon compared to the Arabian Sea? *Geophysical Research Letters*, *29*(24), 88. https://doi.org/10.1029/2002gl016013

Prasanna Kumar, S., Narvekar, J., Kumar, A., Shaji, C., Anand, P., Sabu, P., et al. (2004). Intrusion of the Bay of Bengal water into the Arabian Sea during winter monsoon and associated chemical and biological response. *Geophysical Research Letters*, *31*(15). https://doi.org/10.1029/2004gl020247

Rabalais, N. N., Turner, R. E., Díaz, R. J., & Justić, D. (2009). Global change and eutrophication of coastal waters. *ICES Journal of Marine Science*, *66*(7), 1528–1537. https://doi.org/10.1093/icesjms/fsp047

Rainville, L., Lee, C. M., Arulananthan, K., Jinadasa, S. U. P., Fernando, H. J., Priyadarshani, W. N. C., & Wijesekera, H. (2022). Water mass exchanges between the Bay of Bengal and Arabian Sea from multiyear sampling with autonomous gliders. *Journal of Physical Oceanography*, *52*(10), 2377–2396. https://doi.org/10.1175/jpo-d-21-0279.1

Rao, R. R., & Sivakumar, R. (2003). Seasonal variability of sea surface salinity and salt budget of the mixed layer of the north Indian Ocean. *Journal of Geophysical Research*, *108*(C1), 9. https://doi.org/10.1029/2001jc000907

Saha, U., Siingh, D., Kamra, A. K., Galanaki, E., Maitra, A., Singh, R. P., et al. (2017). On the association of lightning activity and projected change in climate over the Indian sub-continent. *Atmospheric Research*, *183*, 173–190. https://doi.org/10.1016/j.atmosres.2016.09.001

Sahu, G., Mohanty, A. K., Samantara, M. K., & Satpathy, K. K. (2014). Seasonality in the distribution of dinoflagellates with special reference to harmful algal species in tropical coastal environment, Bay of Bengal. *Environmental Monitoring and Assessment*, *186*(10), 6627–6644. https://doi.org/10.1007/s10661-014-3878-3

Sanchez-Franks, A., Webber, B. G. M., King, B. A., Vinayachandran, P. N., Matthews, A. J., Sheehan, P. M., et al. (2019). The railroad switch effect of seasonally reversing currents on the Bay of Bengal high-salinity core. *Geophysical Research Letters*, *46*(11), 6005–6014. https://doi.org/10.1029/2019gl082208

Sathyendranath, S., Jackson, T., Brockmann, C., Brotas, V., Calton, B., Chuprin, A., et al. (2021). ESA ocean Colour Climate Change Initiative (Ocean_Colour_cci): Version 5.0 data [Dataset: Satellite chorophyll]. *NERC EDS Centre for Environmental Data Analysis*. https://doi.org/10.5285/1dbe7a109c0244aaad713e078fd3059a

Sattar, M. A., Kroeze, C., & Strokal, M. (2014). The increasing impact of food production on nutrient export by rivers to the Bay of Bengal 1970–2050. *Marine Pollution Bulletin*, *80*(1–2), 168–178. https://doi.org/10.1016/j.marpolbul.2014.01.017

Seitzinger, S. P., Mayorga, E., Bouwman, A. F., Kroeze, C., Beusen, A. H., Billen, G., et al. (2010). Global river nutrient export: A scenario analysis of past and future trends. *Global Biogeochemical Cycles*, *24*(4). https://doi.org/10.1029/2009gb003587

Sharmila, S., Joseph, S., Sahai, A. K., Abhilash, S., & Chattopadhyay, R. (2015). Future projection of Indian summer monsoon variability under climate change scenario: An assessment from CMIP5 climate models. *Global and Planetary Change*, *124*, 62–78. https://doi.org/10.1016/j.gloplacha.2014.11.004

Subramanian, V. (1993). Sediment load of Indian rivers. *Current Science*, 928–930.

Tanaka, H. L., Ishizaki, N., & Kitoh, A. (2004). Trend and interannual variability of Walker, monsoon and Hadley circulations defined by velocity potential in the upper troposphere. *Tellus A: Dynamic Meteorology and Oceanography*, *56*(3), 250–269. https://doi.org/10.3402/tellusa.v56i3.14410

Thadathil, P., Muraleedharan, P. M., Rao, R. R., Somayajulu, Y. K., Reddy, G. V., & Revichandran, C. (2007). Observed seasonal variability of barrier layer in the Bay of Bengal. *Journal of Geophysical Research*, *112*(C2). https://doi.org/10.1029/2006jc003651

Thirumalaiselvan, P. S., Raman, M., Remya, L., Jayakumar, R., Sakthivel, M., Tamilmani, G., et al. (2023). Monitoring of Harmful Algal Bloom (HAB) of Noctiluca scintillans (Macartney) along the Gulf of Mannar, India using in-situ and satellite observations and its impact on wild and maricultured finfishes. *Marine Pollution Bulletin*, *188*, 114611. https://doi.org/10.1016/j.marpolbul.2023.114611

Thushara, V., Vinayachandran, P. N. M., Matthews, A. J., Webber, B. G., & Queste, B. Y. (2019). Vertical distribution of chlorophyll in dynamically distinct regions of the southern Bay of Bengal. *Biogeosciences*, *16*(7), 1447–1468. https://doi.org/10.5194/bg-16-1447-2019

Tripathy, S. C., Ray, A. K., Patra, S., & Sarma, V. V. (2005). Water quality assessment of Gautami—Godavari mangrove estuarine ecosystem of Andhra Pradesh, India during September 2001. *Journal of Earth System Science*, *114*(2), 185–190. https://doi.org/10.1007/bf02702020

Trott, C. B., Subrahmanyam, B., Murty, V. S. N., & Shriver, J. F. (2019). Large-scale fresh and salt water exchanges in the Indian Ocean. *Journal of Geophysical Research: Oceans*, *124*(8), 6252–6269. https://doi.org/10.1029/2019jc015361

Ueda, H., Iwai, A., Kuwako, K., & Hori, M. E. (2006). Impact of anthropogenic forcing on the Asian summer monsoon as simulated by eight GCMs. *Geophysical Research Letters*, *33*(6). https://doi.org/10.1029/2005gl025336

Umlauf, L., & Burchard, H. (2003). A generic length-scale equation for geophysical turbulence models. *Journal of Marine Research*, *61*(2), 235–265. https://doi.org/10.1357/002224003322005087

Vidya, P. J., Das, S., & MuraliR, M. (2017). Contrasting Chl-a responses to the tropical cyclones thane and Phailin in the Bay of Bengal. *Journal of Marine Systems*, *165*, 103–114. https://doi.org/10.1016/j.jmarsys.2016.10.001

Vinayachandran, P. N. (2009). Impact of physical processes on chlorophyll distribution in the Bay of Bengal. *Indian Ocean biogeochemical processes and ecological variability*, *185*, 71–86. https://doi.org/10.1029/2008gm000705

Vinayachandran, P. N., Murty, V. S. N., & Ramesh Babu, V. (2002). Observations of barrier layer formation in the Bay of Bengal during summer monsoon. *Journal of Geophysical Research*, *107*(C12), SRF19. https://doi.org/10.1029/2001jc000831

Vinayachandran, P. N., & Yamagata, T. (1998). Monsoon response of the sea around Sri Lanka: Generation of thermal domesand anticyclonic vortices. *Journal of Physical Oceanography*, *28*(10), 1946–1960. https://doi.org/10.1175/1520-0485(1998)028<1946:mrotsa>2.0.co;2

Wise, A., Harle, J., Bruciaferri, D., O'Dea, E., & Polton, J. (2022). The effect of vertical coordinates on the accuracy of a shelf sea model. *Ocean Modelling*, *170*, 101935. https://doi.org/10.1016/j.ocemod.2021.101935

Yool, A., Popova, E. E., & Coward, A. C. (2015). Future change in ocean productivity: Is the Arctic the new Atlantic? *Journal of Geophysical Research: Oceans*, *120*(12), 7771–7790. https://doi.org/10.1002/2015jc011167